DARK ENERGY PROBLEM AND POSSIBLE SOLUTIONS

by

Ali Kazım Çamlıbel

B.S., Physics, Boğaziçi University, 2005

Submitted to the Institute for Graduate Studies in
Science and Engineering in partial fulfillment of
the requirements for the degree of
Master of Science

Graduate Program in Physics

Boğaziçi University

2009

DARK ENERGY PROBLEM AND POSSIBLE SOLUTIONS

APPROVED BY:

Assist. Prof. İbrahim Semiz (Thesis Supervisor)	.....
Assist. Prof. A. Savaş Arapoğlu	.....
Prof. Metin Arık	.....

DATE OF APPROVAL: 16.06.2009

ACKNOWLEDGEMENTS

First, I would like to thank my advisor İbrahim Semiz for his guidance and patience throughout the preparing of this thesis. The insights he gave me on a wide range of subjects made this work possible.

I would like to thank my colleague and friend Koray Düztaş for fruitful discussions and for his time. I thank my officemates, especially Arda Halu and Bora Işıldak, for their true friendship in the last eight years.

I also thank Özlem Çalışkan for her love, understanding and support.

Finally, I thank my dear family for their invaluable support and encouragement.

ABSTRACT

DARK ENERGY PROBLEM AND POSSIBLE SOLUTIONS

The end of the twentieth century is marked by a revolutionary discovery in cosmology: The expansion of the universe is accelerating, as revealed by measurements of type Ia supernovae at $z \sim 1$. This most likely means that the energy content of the universe goes beyond that of matter; baryonic or dark. The simplest explanation of this "dark energy" is the cosmological constant Λ, which was originally proposed by Albert Einstein at the beginning of the century to support his static universe model. However Λ is problematic because of its unusually low energy scale and its recent occurrence as the dominant energy component. To overcome these fine-tuning problems alternative theories are proposed, ranging from scalar field theories to braneworld scenarios.

In this thesis, after an introduction to the basic concepts in general relativity and cosmology, we review the recent findings about the universe. Then we go over the alternative theories of dark energy and show how they can be responsible for the late-time cosmic acceleration. We briefly discuss reconstruction of cosmological parameters from data and methods to distinguish between proposed models. The future of the universe is also examined, a classification is given for possible future singularities.

ÖZET

KARANLIK ENERJİ PROBLEMİ VE OLASI ÇÖZÜMLER

Yirminci yüzyılın sonu kozmolojide devrimsel bir keşfe sahne oldu: Tip Ia süpernova ($z \sim 1$) ölçümleri evrenin ivmelenerek genişlediğini ortaya koydu. Bu ivmelenme genel hatlarıyla evrenin enerji içeriğinin sadece baryonik ya da karanlık maddeden oluşmadığı anlamına gelmektedir. Bu "karanlık enerjinin" en basit açıklaması olarak, yüzyılın başında Albert Einstein tarafından statik evren modelini desteklemek için önerilen kozmolojik sabit Λ görülebilir. Öte yandan Λ, alışılmadık derecede düşük enerji seviyesiyle ve baskın enerji bileşeni olarak ortaya çıkış zamanı açısından problemler doğurmaktadır. Bu ince ayar problemlerinin üstesinden gelmek için skaler alan teorilerinden zardünya senaryolarına uzanan alternatifler ileri sürülmüştür.

Bu tezde, genel görelilik ve kozmolojideki temel kavramları tanıttıktan sonra evren hakkındaki son bulguları gözden geçiriyoruz. Ardından alternatif karanlık enerji teorilerini ve geç dönem bir ivmelenmeye nasıl sebep olabileceklerini tartışıyoruz. Kozmolojik parametrelerin verilerden yeniden inşasını ve önerilen modelleri birbirinden ayırt etmenin metodlarını kısaca irdeliyoruz. Son olarak evrenin geleceğini inceleyip, olası gelecek tekilliklerinin bir sınıflandırmasını yapıyoruz.

TABLE OF CONTENTS

ACKNOWLEDGEMENTS iii
ABSTRACT iv
ÖZET v
LIST OF FIGURES viii
LIST OF SYMBOLS/ABBREVIATIONS xi
1. INTRODUCTION 1
2. COSMOLOGY BEFORE 2000 8
2.1. Basics of General Theory of Relativity 8
2.2. Einstein Static Universe and Cosmological Constant 10
2.3. The Expanding Universe 11
2.4. Dark Matter 16
2.5. Inflation 18
2.6. Measuring the Universe 20
3. RECENT OBSERVATIONS 27
3.1. Flatness of the Universe 27
3.2. Accelerated Expansion and Dark Energy 30
4. DARK ENERGY CANDIDATES 39
4.1. Cosmological Constant Revisited 39
4.2. Quiessence 40
4.3. Quintessence 40
4.4. K-essence 43
4.5. Spintessence 46
4.6. Phantom Dark Energy 48
4.7. Chaplygin Gas 50
4.8. Other Models 51
5. OTHER POSSIBILITIES 52
5.1. Modified Gravity 52
5.2. Braneworld Models 53
5.3. Backreaction of Cosmological Perturbations 55

6. COMPARING DARK ENERGY MODELS WITH OBSERVATIONS 58
6.1. The "Reconstruction" of Dark Energy Properties 58
6.2. Statefinder Diagnostic 59
7. FUTURE OF THE UNIVERSE 66
8. CONCLUSIONS AND PROSPECTS 70
APPENDIX A: MATHEMATICAL DEFINITIONS AND CONVENTIONS . . 72
APPENDIX B: SCALAR FIELD IN COSMOLOGY 74
B.1. Quintessence 74
B.2. K-essence 75
B.3. Spintessence 77
APPENDIX C: COSMOLOGY ON A BRANE IN A 5D BULK 79
APPENDIX D: DERIVATIONS REGARDING STATEFINDER PARAMETERS 81
REFERENCES 84

LIST OF FIGURES

Figure 2.1. The Einstein static universe and its instability 14

Figure 2.2. Matter-dominated universe must be dynamic without the cosmological constant 15

Figure 2.3. A typical rotation curve for spiral galaxies. 17

Figure 2.4. Two points A and B which are observed by P to be in thermal equilibrium are not allowed to be in causal connection in standard Big Bang model. 18

Figure 2.5. Having an exponential expansion for an interval $\Delta t_{\rm inf}$ instead of a radiation driven one ($a(t) \propto t^{1/2}$), causes a dilation $\sim \exp(H\Delta t_{\rm inf})$ in conformal time $\Delta\eta = \int \frac{cdt}{a(t)}$, pushing Big Bang line further into the past in terms of η. 20

Figure 2.6. Plots showing the expansion characteristics for different amounts of contribution in a "Λ - Cold Dark Matter" two-fluid model (adopted from [11]). 25

Figure 3.1. Dipole anisotropy based on 4-year mission of COBE. Image is published by COBE Science Working Group. 27

Figure 3.2. WMAP5 picture of CBR showing temperature fluctuations with a resolution of 10^{-4}K. Darkest regions are coldest ones. Image is published by WMAP Science Team. 28

Figure 3.3. Angular power spectrum analysis of WMAP5 data. Image is published by WMAP Science Team. 30

Figure 3.4. Angular size of the observed region depending on curvature. . . . 31

Figure 3.5. Too faint SNe Ia means expansion of the universe is accelerating . 32

Figure 3.6. Data from Supernova Cosmology Project, together with various theoretical $d_L(z)$-curves (adopted from [22]). 33

Figure 3.7. Constraints on the energy composition of our universe by the Supernova Cosmology Project (adopted from [22]). 34

Figure 3.8. "Gold data" plotted over the best fit for a flat cosmology with $\Omega_M = 0.27$ and $\Omega_\Lambda = 0.73$ (adopted from [23]). 37

Figure 3.9. First year data from Supernova Legacy Survey with various cosmological models (adopted from [24]). 38

Figure 4.1. "Tracker" quintessence models: Dashed line represents radiation density where dotted-dashed line is matter density. Solid curve is for quintessence "tracker". 42

Figure 5.1. It can be clearly seen that model enters a negative deceleration regime. 56

Figure 6.1. Parametric reconstruction of $w(z)$ with an ansatz of the form $H(z) = H_0(\Omega_M(1+z)^3+A_1+A_2(1+z)+A_3(1+z)^2)^{(1/2)}$ where $A_1+A_2+A_3 = 1-\Omega_M$. Thick solid line is the best fit ($\Omega_M = 0.3$). 1σ and 2σ confidence levels are given by light grey and dark grey areas (adopted from [54]). 60

Figure 6.2. Nonparametric reconstruction of $w(z)$. Vertical lines show 1σ and 2σ confidence levels (adopted from [55]). 61

Figure 6.3. Parametric reconstruction of $w(z)$ with an ansatz $w(z) = w_0 + w_1 \frac{z}{1+z}$. Blue line is the best fit ($w_0 = -1.212$, $w_1 = 0.839$) and light grey and dark grey areas represent 68% and 95% confidence levels (adopted from [56]). 61

Figure 6.4. r-s evolution of pure Chaplygin universe 63

Figure 6.5. r-s evolutions of Chaplygin gas and Dust for different amounts of contribution 64

Figure 6.6. Left panel exhibits "r-s" plots for three different dark energy families. Chaplygin gas curves, (upper-left) are identical to ours. On the lower-right we see fluids with constant w (quiessence) with constant $s = 1 + w$ and r going down asymptotically to $1 + \frac{9}{2}w(1 + w)$. Quintessence curves, solid ones on the lower half, are from model described in (4.9). Depending on α, they all have a monotonically decreasing s, where r decreases from unity to a minimum then rises back. Right panel shows same families in a "r-q" diagram (adopted from [57]). 65

Figure 6.7. Thick solid curve in BRANE2 section is the one we discussed in (5.13) (adopted from [57]). 65

LIST OF SYMBOLS/ABBREVIATIONS

a	Scale factor
A	Chaplygin gas parameter
c	Speed of light
d_H	Horizon distance
d_L	Luminosity distance
$g_{\mu\nu}$	Metric tensor
$G_{\mu\nu}$	Einstein tensor
G	Gravitational constant
H	Hubble parameter
I	Observed intensity
k	Curvature parameter
L	Actual luminosity
$M_{\rm pl}$	Planck mass
p	Pressure
q	Deceleration parameter
r	First statefinder parameter
R	Ricci scalar
$R_{\mu\nu}$	Ricci tensor
$R^{\alpha}_{\beta\gamma\delta}$	Riemann curvature tensor
s	Second statefinder parameter
S	Action
$t_{\rm dec}$	Time of decoupling
$T_{\mu\nu}$	Stress-energy-momentum tensor
V	Potential energy of a scalar field
w	Equation of state parameter
X	Kinetic energy of a scalar field
z	Redshift

$\Gamma^{\alpha}_{\beta\gamma}$	Christoffel symbol
η	Conformal time
θ	Phase of the complex field
κ	Coupling constant in Einstein's equations
Λ	Cosmological constant
ρ	Energy density
ϕ	Magnitude of the scalar field
Φ	Complex scalar field
Ω	Energy density fraction

BB	Big Bang
CBR	Cosmic background radiation
CDM	Cold dark matter
COBE	Cosmic Background Explorer
DE	Dark energy
DGP	Dvali-Gabadadze-Porrati
DM	Dark matter
EFE	Einstein field equations
FRW	Friedmann-Robertson-Walker
GUT	Grand unified theory
IRAS	Infrared Astronomical Satellite
JDEM	Joint Dark Energy Mission
SCP	Supernova Cosmology Project
SNe Ia	Type Ia supernovae
WIMP	Weakly interacting massive particle
WMAP	Wilkinson Microwave Anisotropy Probe
WMAP5	WMAP 5-year data

1. INTRODUCTION

Our perception of the universe has evolved throughout history, with observations being the foundation of new theories. In astronomy, new observations are usually possible only with new observational methods. Therefore, new instruments have often caused important discoveries, even scientific revolutions.

The first instrument of astronomical observation was the naked eye, the "observatories" being mainly structures to house the astronomers and maybe shield their eyes from terrestrial light and guide their gaze. The equipment consisted of apparatus to measure angles, and time.

Naked-eye observations suggested a geocentric model of heavens, culminating with Ptolemy (2^{th} century A.D.). The Ptolemaic model, where the universe "ended" at the celestial sphere containing the fixed stars, was the dominant theory through the medieval ages, although sporadic suggestions for heliocentric models existed too. The most notable of these was Aristarchus (3^{th} century B.C.), whose model was unable to overcome the objections of the Aristotelians.

Naked-eye techniques were perfected by the Danish astronomer Tycho Brahe, whose data (1572-1601) were precise enough for Kepler (1601-1623) to rule out the Ptolemaic model. The heliocentric idea had been resurrected by Copernicus in 1543, but Kepler found that the Copernican model with its Ptolemy-like circles was also ruled out. Finally, he found that Tycho's data could be summarized in very simple form by the now very well-known Kepler's laws involving elliptical orbits with the Sun at one of the foci.

When Newton formulated his law of gravitation, these elliptical orbits were shown to be one solution of the equations of motion, demonstrating the universal nature of gravitation; a true revolution.

The first improvement over the naked eye as an astronomical instrument was Galileo's primitive telescope. With it the Milky Way was observed to resolve into stars. Since the need for the celestial sphere is removed by the heliocentric revolution, the natural corollary is that stars invisible to naked eye could be far away, and the universe therefore bigger than previously thought.

The natural extension of this idea is that the universe could be infinite. The extension of the heliocentric idea, that the Earth is not special, is that there is no special point in the universe at all, i.e. the universe should be uniform. Since no dynamics could be observed or conceived for the universe as a whole, it came to be held that the universe may be static, therefore eternal, as well.

Olbers' Paradox showed that the universe could not have all these three properties together; the darkness of the night sky tells us that.[1] In some sense, Olbers' Paradox could be said to constitute the beginning of modern cosmology, since it is the first irrefutable statement about the universe.

The telescopes, improving steadily since Galileo, reached the ability to look beyond the Milky Way in the beginning decades of the last century (In fact, the very idea of "our galaxy" was observationally established only in the second decade). Moreover, the telescopes acquired the ability of analysing light, in addition to collecting it – in other words, spectroscopy was added to the tools of observational astronomy. The presence of various line patterns in the spectrum of an object told astronomers about the chemical makeup of that object, the overall shift of those lines told the speed of the object relative to the Earth. The speeds measured for other galaxies, combined with various methods of distance estimation in the work of Edwin Hubble (1929) gave the single most important fact about the universe: It is expanding.

[1] In a uniform, static and eternal universe number of light sources (stars) at a distance r is proportional to the volume element $4\pi r^2 dr$. Intensity of one source may be given by $I = \frac{C}{4\pi r^2}$ where C is a constant. So total intensity from a shell with thickness dr is Cdr, and total observed intensity on Earth will be $\int_0^\infty Cdr \longrightarrow \infty$, which predicts a night sky completely bright, conflicting with reality.

On the theoretical side, general relativity was formulated by Einstein during 1905-1915. This theory requires that the universe be described by a so-called metric. When one puts the idea that the universe should be homogeneous and isotropic, called the "cosmological principle" (the almost philosophical extension of the heliocentric idea) into this form, one finds that the space geometry of the universe is restricted to one of three possibilities, called open, flat and closed, respectively; where the flat case is really the borderline between the open and closed cases. Moreover, general relativity ties the evolution of the universe to its matter content, and under reasonable assumptions the universe must be dynamic in all three cases. But, Einstein modified his theory just to avoid this, introducing the cosmological constant, and constructed his static universe model (discussed in Chapter 2). He reverted to the original form of general relativity after Hubble's discovery.

But, general relativity was far from being generally accepted, since it is difficult to test experimentally. In fact, for a while, the dominant theory of cosmology was flatly in contradiction with general relativity. This theory, called Steady State cosmology, held that the local properties of the universe should not change with time. Since by then, the expansion of the universe was an established observational fact, this theory necessitated continuous creation of matter, violating conservation of mass-energy. Although it was argued that the violation was undetectably small locally, it goes against the very spirit of general relativity, where mass-energy conservation is built-in.

In a general relativistic model however, the local properties of the universe evolve with time. In particular; the universe is expected to become denser and hotter as one follows this evolution into past. George Gamow realized that at some point in time, the universe would become a plasma –therefore opaque to light– and further in the past, it would become hot enough for nuclear reactions. These reactions would leave their imprint in chemical makeup of the universe, (in addition to causing the idea to be branded as "Big Bang" by its detractors, since nuclear reactions brought bombs to mind) detectable today. The transition from opaqueness to transparency as the expanding universe cools would set free ("decouple") large number of photons *with a thermal spectrum*, which also would be theoretically detectable today at redshifted

wavelengths/temperature.

And detected it was, in 1964, with the help of a microwave antenna designed for space communications; another demonstration of new observational techniques opening up new vistas (or closing off some paths of thought). With the discovery of the Cosmic Background Radiation ("CBR")[2] , the Steady State cosmology was largely abandoned and the Big Bang became dominant, general relativity providing the framework for describing or understanding the global properties of the universe.

Now, since the universe was understood to be dynamic, the attention was also focused on the future behaviour of the universe. The energy density of the CBR being negligible compared to that of stars and galaxies, the latter were seen as the dominating content of the universe. Under these assumptions general relativity ties the density, spatial geometry and fate of the universe together: An open universe will expand forever, whereas a closed one will recollapse in the so-called "Big Crunch". The open/forever universe will be realized if the density is below a critical value, the closed/recollapse universe if it is above (Section 2.3). So, a measurement of the density of the universe was imperative.

Astronomers knew how to estimate the masses of stars; and their density, even after combination with the density of interstellar material detected by their emissions or absorptions of electromagnetic radiation, fell far short of the critical value dividing the open/forever and closed/recollapse universes.

But, mass can also be measured by investigating its effect on the motion of test objects –for example, the Earth's mass can be determined by looking at the motion of the Moon, without knowing the mass of the Moon. This approach gave densities that were consistently higher than the density of matter detected directly. Since direct detection involves emission/absorption of electromagnetic radiation, this type of matter is called *luminous* matter, whereas the nonluminous matter was called *dark matter* in

[2]In literature this radiation is often referred to as Cosmic Microwave Background ("CMB") Radiation, but we prefer to call it CBR, because it was not always peaked in the microwave band.

contrast (Section 2.4).

The fundamental matter particles in the standard model of particle physics are mostly charged (except the neutrinos), hence they should interact with electromagnetic radiation. Therefore the presence of dark matter is a problem of large magnitude: There seems to be more unknown matter in the universe than known matter, pointing towards possible inadequacy of the standard model of particle physics, and interestingly tying the physics of very small together with the physics of the very large.

The problem was exacerbated by the advent of the Inflation scenario, put forward to solve some fine-tuning problems of the standard Big Bang theory (Section 2.5). The so-called horizon, flatness and monopole problems are solved by introducing a period of exponential expansion, resulting in an exactly flat universe today –therefore leading to the expectation that the density of the universe is equal to the critical density. Since luminous matter has only 5% of this density, an overwhelming fraction of the matter in the universe seemed to be dark.

Newer telescopes, able to peer much deeper into the universe –therefore much farther into the past– brought a new twist to the story: Using very far supernovae as *standard candles*, it was determined that the expansion of the universe is *accelerating*. This result was a stunning surprise to almost everyone concerned, since the combination of standard general relativity and normal/dark matter is attractive. Since the dark matter concept already had put the matter part of the argument in doubt, acceleration is generally interpreted as pointing to the existence of another kind of source, although ideas for modifying general relativity also exist. The needed property of this source (negative pressure) seems too strange for matter, and it is undetectable electromagnetically, so it was called *dark energy*. The dark energy concept decreases the magnitude of dark matter problem, at the cost of a new and possibly more confounding problem: The latest estimate for the content of the universe is 5% normal matter, 25% dark matter and 70% dark energy.

In this work, we will describe the problem of dark energy, together with the ideas/observations that preceded and eventually led to it, and we will also describe suggested solutions.

In Chapter 2 we present a discussion of cosmology up to roughly the year 2000 setting up notation and introducing relevant concepts in the process. First we introduce Einstein's general relativity and examine the first use of cosmological constant as the Einstein static universe. Then we construct the mathematical basis for an expanding universe, focusing in particular on the matter-dominated expansion which was thought to be the case. This leads to discussion of dark matter and the inflationary scenario. At the end of the chapter we show how one can measure the expansion through the observable parameters redshift and luminosity distance.

In Chapter 3 we will go over the observations made in the last two decades which formed the idea of dark energy; flatness of the universe from anisotropy of CBR and accelerated expansion from type Ia supernovae data.

Dark energy candidates are discussed in Chapter 4. First we will revisit cosmological constant as the natural solution to the problem and see if there are implications to it. Then we will look for other possibilities for a dark fluid such as scalar field dark energy (quintessence, k-essence, spintessence), the possibility called phantom energy and a fluid with exotic equation of state (Chaplygin gas).

Chapter 5 is about the explanations to accelerated expansion other than the dark energy. We will focus on modified gravity, braneworld models and the idea that cosmological perturbations may give the impression of acceleration.

In Chapter 6 we will see how to reconstruct cosmological parameters from data. Then we are going to introduce statefinder pair –variables which can also be reconstructed from data and calculated for any proposed model– a useful diagnostic for future observations.

We will talk about the future of a dark energy dominated universe in Chapter 7. We will focus on the fate of the galaxies as possible island universes and give a summary of possible future singularities.

2. COSMOLOGY BEFORE 2000

2.1. Basics of General Theory of Relativity

At the beginning of the 20^{th} century when Einstein constructed general theory of relativity, there was limited interest in developing a new theory for gravity. Newton's law of gravitation was problematic in the manner that it asserts instantaneous action at a distance, even Newton himself was not comfortable with this notion stating that he never assigned the cause of this force but what it does. However the theory continually turned out to be in agreement with the observations except for a small discrepancy in the precession of the perihelion of planet Mercury.

Newtonian formalism of gravity, as opposed to the other natural forces, had a distinctive feature; inertial mass, which determines the response to the attraction, is also the source of the force. This fact, which was there in Newtonian theory but did not constitute new physics, leads to "the principle of equivalence"; prominent idea beneath the general theory of relativity:

"The motion of a particle in a gravitational field is independent of its mass and composition" [1, Page 1050].

It may also be stated in its generalized form,

"A frame linearly accelerated relative to an inertial frame is locally identical to a frame at rest in a gravitational field" [1, Page 386].

As a result gravitation may be treated as a solely geometrical phenomenon in which matter does not move under the sway of a force field but flows on geodesics of spacetime. Distribution of energy and momentum determines the curvature of those geodesics. For an adequate geometrical formulation one should introduce the Riemannian geometry for 3+1 dimensional spacetime described by the metric $g_{\mu\nu}$, a set of

coefficients in the line element showing the spacetime interval in terms of coordinate differentials,

$$ds^2 = g_{\mu\nu} dx^\mu dx^\nu \tag{2.1}$$

where sum over indices μ and ν is implied.[3] The metric coefficients $g_{\mu\nu}$ constitute a tensor, and out of the metric and its first and second derivatives the Riemann and Ricci tensors can be constructed, as is well-known in differential geometry.[3]

General theory of relativity associates a stress-energy-momentum tensor with a spacetime, and simple guidelines lead to a set of 10 coupled differential equations,

$$G_{\mu\nu} = \kappa T_{\mu\nu}. \tag{2.2}$$

Written in tensor form, they are called Einstein Field Equations ("EFE"). $G_{\mu\nu}$ is the Einstein Tensor given by

$$G_{\mu\nu} = R_{\mu\nu} - \frac{1}{2} R g_{\mu\nu}, \tag{2.3}$$

where $R_{\mu\nu}$ is the Ricci tensor, and R the curvature scalar.[3]

$T_{\mu\nu}$ is stress-energy-momentum tensor or simply energy-momentum tensor; putting it on the right hand side of the equations as the source it replaces its Newtonian counterpart, inertial mass. By doing so general relativity states that gravity couples not only to inertial mass but to a variety of physical quantities such as energy and momentum.

κ is the coupling constant, given in SI units by $\frac{8\pi G}{c^4}$, although frequently unit systems are used where $G = 1$, $c = 1$. Solving EFE means finding a metric tensor $g_{\mu\nu}$ that satisfies Equation 2.2 for a specified or physically reasonable form of $T_{\mu\nu}$.

The first solution to Einstein's equations came from Schwarzschild. Dealing with

[3]Definitions and conventions are given in Appendix A.

the vacuum field equations ($T_{\mu\nu} = 0$), it described the spacetime near a massive object. It is represented by the line element,

$$ds^2 = -\left(1 - \frac{2GM}{c^2 r}\right) c^2 dt^2 + \frac{1}{1 - \frac{2GM}{c^2 r}} dr^2 + r^2(d\theta^2 + \sin^2\theta d\phi^2). \tag{2.4}$$

This surprisingly simple solution, from which the precession of the perihelion of planets and deflection of light by a star can be predicted, served as one of the early tests of general relativity.

2.2. Einstein Static Universe and Cosmological Constant

Before the emergence of general relativity, the universe was considered to be static and homogeneous. (See Chapter 1) But as will be shown in the next section, the model predicted by general relativity indicates that it must be dynamic.

Einstein immediately tried to construct a model, in which universe does not undergo a large-scale motion, sticking to the old tradition. To obtain this he relaxed the condition that the flat space should be empty by introducing a constant in his equations. With this modification field equations became [2]

$$G_{\mu\nu} + \Lambda g_{\mu\nu} = \kappa T_{\mu\nu}. \tag{2.5}$$

Λ is the cosmological constant mentioned in Chapter 1. It may be inserted also into the right hand side of the equation and interpreted as the vacuum $T_{\mu\nu}$:

$$G_{\mu\nu} = \kappa(T_{\mu\nu} - \frac{\Lambda}{\kappa} g_{\mu\nu}). \tag{2.6}$$

This constant, bringing about a cosmological repulsion opposing the gravitational attraction, was useful to construct a static universe model, but the model is an unstable one under small perturbations; a slight contraction will result in a gravitational collapse whereas an expansion would decrease the gravitational attraction and the system

will expand indefinitely (See Figure 2.1).

However, Einstein's attempt may be seen as the first universe model in the history of modern cosmology, with the use of general relativity and the cosmological principle, that is, the assumptions of the universe to be isotropic and homogeneous.

The cosmological constant was put away by Einstein twelve years after its invention, referring to it as his "biggest blunder", with the discovery of the expansion of the universe.

2.3. The Expanding Universe

Expanding characteristics of the universe are observed by Edwin Hubble and published in 1929 after 10 years of observation [3]. The statement is that the distance and the recessional velocity of an object in deep space are proportional to each other. This can be summarized by the Hubble's law

$$v = Hd, \tag{2.7}$$

where H is the Hubble parameter (sometimes inaccurately called the Hubble constant).

However from cosmological point of view these concepts of "distance" and "recessional velocity" can be misleading, therefore they should be studied carefully and maybe replaced by other quantities (see Section 2.6).

The suitable theoretical basis for an expanding universe in the context of general relativity came earlier than the publication of observational evidence. In 1922 Friedmann presented his solution of Einstein's equations for a dynamical universe [4] in the form of

$$ds^2 = -c^2dt^2 + a^2(t)\left[\frac{dr^2}{1-kr^2} + r^2(d\theta^2 + \sin^2\theta d\phi^2)\right]. \tag{2.8}$$

This is the famous Friedmann-Robertson-Walker ("FRW") metric where $a(t)$ is called the scale factor; a parameter representing the relative expansion of the universe. From here we can define Hubble parameter as

$$H = \left(\frac{\dot{a}}{a}\right). \tag{2.9}$$

Here k is a variable which may take values of 1, 0 or -1, each bringing about the line element for the spatially closed, flat or open universes respectively.

FRW metric can be substituted in the left-hand side of the Einstein's equations. For the right-hand side it is appropriate to choose a perfect fluid with energy density ρ and pressure p whose energy-momentum tensor is in the following form,

$$T_{\mu\nu} = \frac{(\rho + p)}{c^2} u_\mu u_\nu + p g_{\mu\nu}, \tag{2.10}$$

where u_a is the 4-velocity. Cosmological principle tells us matter is at rest, therefore $u^i = 0$ and $u^0 = c$.

So the Einstein's equations with the cosmological constant Λ give,

$$\left(\frac{\dot{a}}{a}\right)^2 + \frac{kc^2}{a^2} - \frac{\Lambda c^2}{3} = \left(\frac{8\pi G}{3c^2}\right)\rho, \tag{2.11}$$

$$2\frac{\ddot{a}}{a} + \left(\frac{\dot{a}}{a}\right)^2 + \frac{kc^2}{a^2} - \Lambda c^2 = -\left(\frac{8\pi G}{c^2}\right)p. \tag{2.12}$$

Combining these two one gets

$$\frac{d}{dt}(a^3\rho) = -p\frac{d}{dt}(a^3), \tag{2.13}$$

an equation corresponding to the conservation of energy for an adiabatic volume change

in thermodynamical context. It automatically follows that,

$$\dot{\rho} = -3H(\rho + p). \tag{2.14}$$

A perfect fluid can be characterized by the relation between its energy density and pressure, namely by its equation of state. In cosmology it is usually taken to be of the form

$$p = w\rho. \tag{2.15}$$

The parameter w may take different values depending on the type of the fluid. For example it is 0 for pressureless dust, the fluid filling the universe in a matter-dominated model; and $\frac{1}{3}$ for a universe dominated by isotropic radiation. If the universe is filled with more than one fluid where the different components do not interact with each other, Equation 2.13 is still valid for each component separately, because it is really energy conservation (it could be derived from ${T^{\mu\nu}}_{;\nu} = 0$).

For a fluid with equation of state parameter w, (2.13) will give

$$\rho \propto a^{-3(1+w)}. \tag{2.16}$$

If the universe is dominated by a single such fluid and if $k = 0$, we can put this into (2.11) and get

$$a \propto t^{\frac{2}{3(1+w)}}. \qquad \text{[for } k = 0\text{]} \tag{2.17}$$

The "fluid" of galaxies that seems to be constituting the dominant matter in the universe is equivalent to a "dust fluid", i.e. $p = 0$. Then we can get from (2.13) that ρ is proportional to $(1/a^3)$ and it is possible to construct an energy conservation-like

law by rearranging (2.11) as

$$\dot{a}^2 - \frac{\Lambda c^2}{3}a^2 - \frac{8\pi G}{3c^2}\frac{\rho_0 a_0^3}{a} = -kc^2, \tag{2.18}$$

where $\dot{a}^2$ corresponds to the kinetic term and $-\frac{\Lambda c^2}{3}a^2 - \frac{8\pi G}{3c^2}\frac{\rho_0 a_0^3}{a}$ may be treated as an effective potential. One can easily see from the effective potential diagram in Figure 2.1 that if k is positive this model has a static solution, which corresponds to Einstein static universe. But one can equally well see from the figure that this solution is unstable in small perturbations.

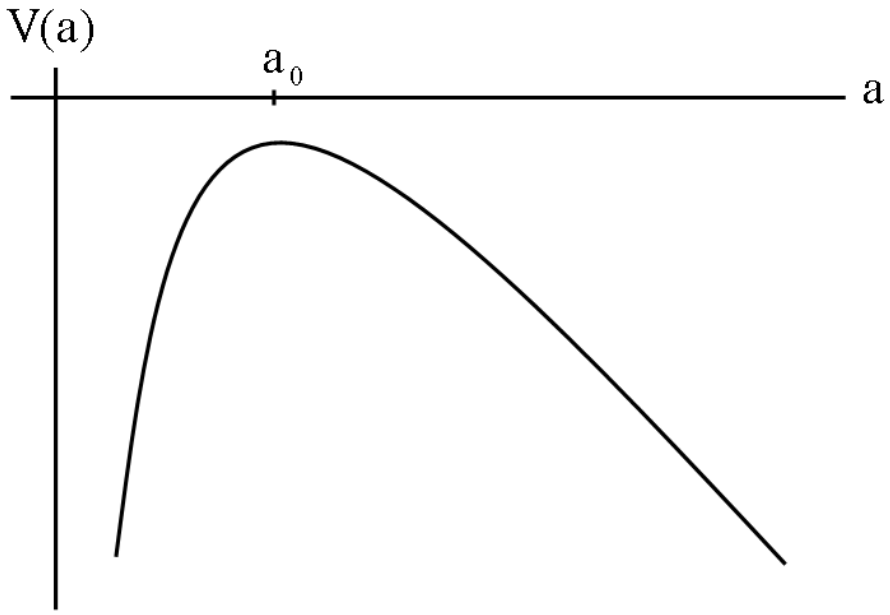


Figure 2.1. The Einstein static universe and its instability

On the other hand if one excludes the cosmological constant, there is no static solution. (Figure 2.2)

As mentioned in the first chapter, the idea of Big Bang is based upon the evolution of local properties of the universe with time; at some point in the past radiation density will dominate over matter density and the universe will be hot; hot enough for thermonuclear reactions. This idea gained acceptance with the detection of CBR [5]; the 2.7K black-body radiation left over from the radiation-dominated early universe.

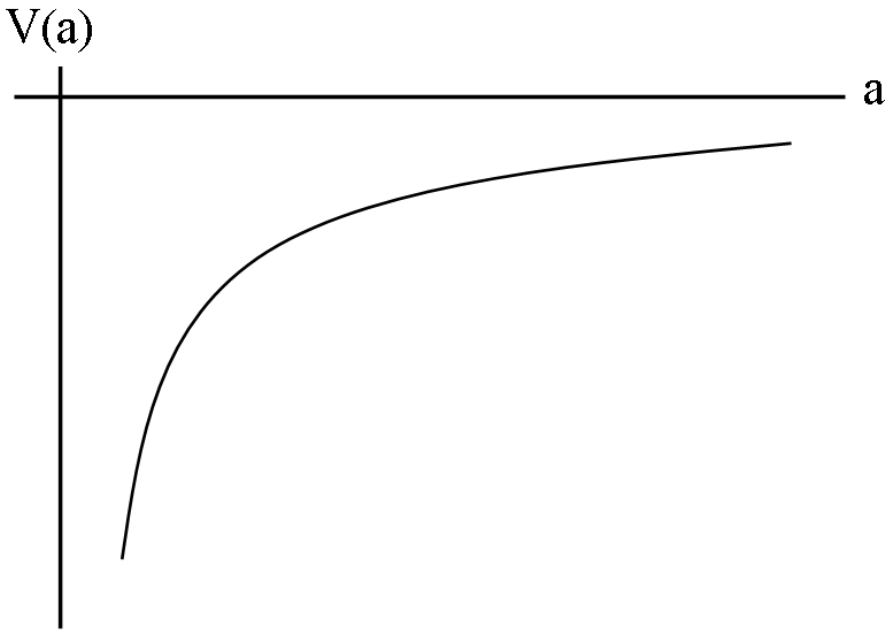


Figure 2.2. Matter-dominated universe must be dynamic without the cosmological constant

This statement about the past of the universe does not depend very much on how much or what kind of matter there is in the current universe. The future of the universe on the other hand, depends on the density and composition of its content.

In a matter-dominated universe which was the accepted case throughout the 20^{th} century, the expansion rate decreases due to gravitational attraction. Examining (2.11) one can see that there is a critical value of density,

$$\rho_c = \frac{3c^2}{8\pi G}\left(\frac{\dot{a}}{a}\right)^2, \tag{2.19}$$

where k is 0 and hence universe is flat. Defining

$$\Omega \equiv \frac{\rho}{\rho_c}, \tag{2.20}$$

one can identify three cases.

For Ω=1 the universe is flat and its expansion rate will approach zero asymptot-

ically, never reaching it. If $\Omega > 1$ then the universe is closed, which eventually will collapse under gravitation; the infamous "Big Crunch" scenario. For the $\Omega < 1$ case the universe is open and experiences a decelerating but continuing expansion. These cases correspond to the "energy" being zero, negative and positive respectively, in Figure 2.2.

So, what was needed now was a measurement of Ω; or, density of the universe. The stars and the interstellar gas/dust gave only a few percent of critical density, but when masses of the same galaxies were estimated by looking at their gravitational effects, larger values were always found. These led to the concept of *dark matter* not detectable otherwise.

2.4. Dark Matter

The first realization of a "dark" component contributing to the energy density of the universe dates back to 1930's [6, 7]. Observed velocities of galaxies in a cluster turned out to be much higher than the values estimated for a "visible mass only" composition. This excess in the mass to light ratio was attributed to some dark matter, which does not interact electromagnetically but gravitationally.

Next evidence came much later with the measurement of rotation curves of spiral galaxies through the late 1960's and early 1970's (Figure 2.3). If the galaxy's mass distribution coincided with its light distribution, the rotational velocity of the interstellar gas graphed in Figure 2.3 should go down as $\frac{1}{\sqrt{r}}$ after the optical extent. But the curve stays flat well beyond the optical extent, indicating the presence of dark matter. In fact, it is found that dark matter dominates in the galaxy and its distribution is approximately spherically symmetric, so it is said the galaxy (whose optical components mainly lie in a disk) is embedded in a "dark matter halo".

Dynamical investigations in the spirit of the measurements of galaxy rotation curves can show the presence of matter on scales they probe or smaller, but not larger. So we know that some dark matter is clustered in and around the galaxies, while there

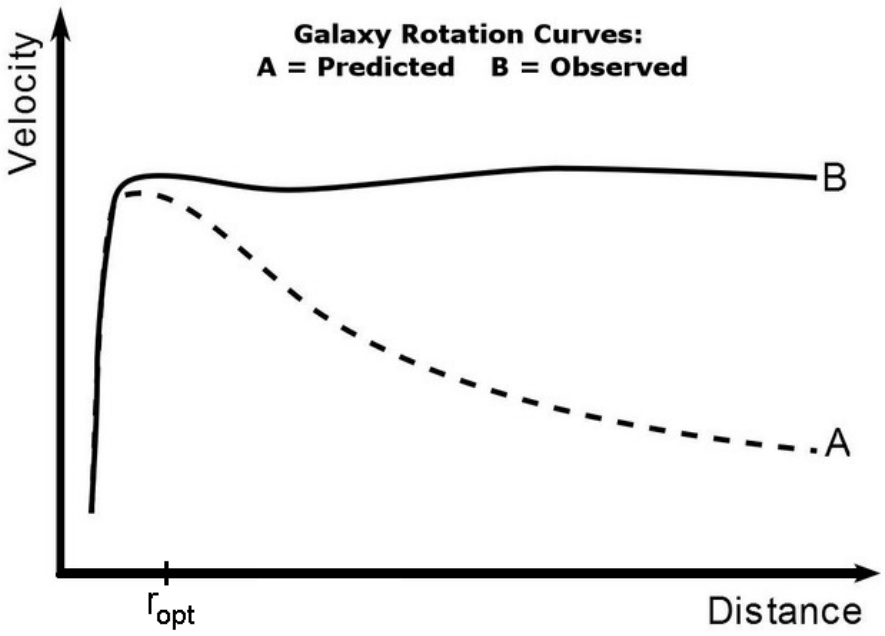


Figure 2.3. A typical rotation curve for spiral galaxies.

is also diffuse intergalactic dark matter. Relativistic particles could not be confined by the gravitational well of a galaxy, so the unclustered part of dark matter is called hot dark matter (neutrinos being a good example [8, Page 204]), and the clustered part cold dark matter. To be more precise, the dark matter components are called hot or cold, depending on if they were relativistic or nonrelativistic when they decoupled from the rest of the content of the universe, because then, cold dark matter ("CDM") plays a role in the formation of structure in the universe.

Most popular candidates for CDM are axion –an elementary particle predicted in an extension of quantum chromodynamics– and a class of particles called WIMP's (weakly interacting massive particle) which may arise in various theories like super-symmetry or universal extra dimensions. There is also a claim of direct detection of WIMP's [9], which is not confirmed by other experiment.

Most recently it is shown that there exists a dark disc in galaxies alongside the dark halo [10].

2.5. Inflation

Throughout the 70's when Big Bang theory became mainstream, modern cosmology faced some shortcomings, usually referred to as the horizon, flatness and monopole problems. As a possible solution of these problems, the inflationary scenario was proposed, which naturally results in $\Omega = 1$ (or very close to it) today. This means that the contribution of dark components to the energy density of the universe is even larger than what the dynamical measurements suggest.

The *horizon problem* refers to the equality of the CBR temperature in diametrically opposite regions in the sky, which could not have had causal interaction in the time between the Big Bang and decoupling (Figure 2.4).

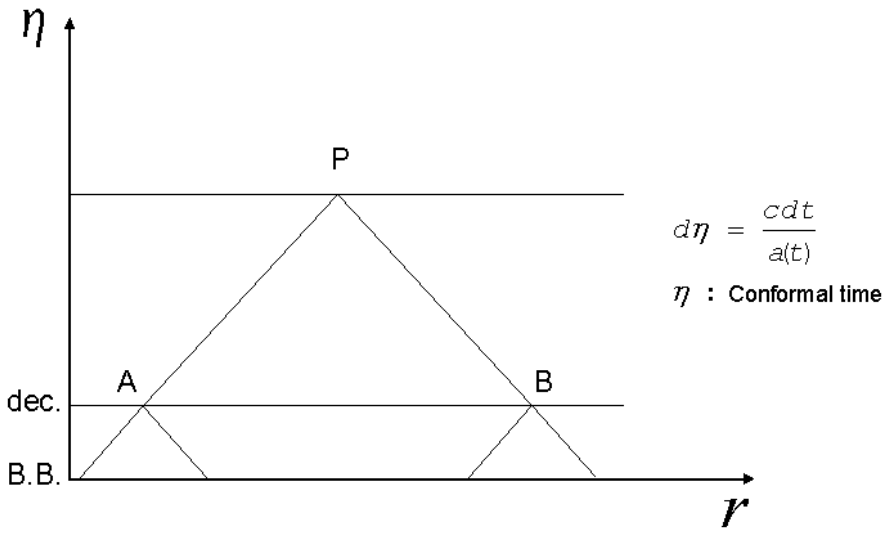


Figure 2.4. Two points A and B which are observed by P to be in thermal equilibrium are not allowed to be in causal connection in standard Big Bang model.

The *flatness problem* is the fine-tuned value of the density of the universe which is very close to the critical density resulting in a flat universe. Deviations from critical density may be written using Equation 2.11 as

$$(\Omega^{-1} - 1) = -\frac{3c^4 k}{8\pi G \rho a^2}. \tag{2.21}$$

So, for radiation dominated era ($\rho \propto a^{-4}$), these deviation grow with a^2, where for matter dominated era ($\rho \propto a^{-3}$), they grow with a. If one considers the age of the universe, even slightest deviation from the critical density in early times would correspond to a huge deviation today. Hence one may conclude that curvature is very sensitive to initial conditions and observed flatness is a problem in standard Big Bang model.

Thirdly, there is *monopole problem*; early universe after the Big Bang was very hot, so that stable and heavy magnetic monopoles should be produced as topological defects in the spontaneous symmetry breaking during the phase transitions in the expanding, therefore cooling universe. These phase transitions are predicted in grand unified theories. These monopoles, being very massive, should go nonrelativistic early and therefore dominate the energy density of the universe today. However, all searches up to date have returned no clue about such particles.

The inflationary scenario postulates a period of exponential expansion in the very early history of the universe. This expansion is caused by the universe temporarily having equation of state $p = -\rho$. This equation of state is valid for the time when the universe is caught in a "false vacuum", i.e. the phase transition mentioned in the context of the monopole problem happens not adiabatically but with a delay. Inflation is thought to have lasted for about 100 e-foldings.

During inflation a small and causally connected region may expand into the entire observable universe today which solves the horizon problem at first glance (Figure 2.5).

The flatness problem is also solved, since during exponential growth curvature term is reduced by a factor 10^{52} leaving Ω very close to unity at the end of inflation. This means that in a matter-dominated universe, more than 90% of the matter in the universe would be dark.

Magnetic monopoles created in hot early universe are diluted during inflation; their number density will fall exponentially, which explains their absence today.

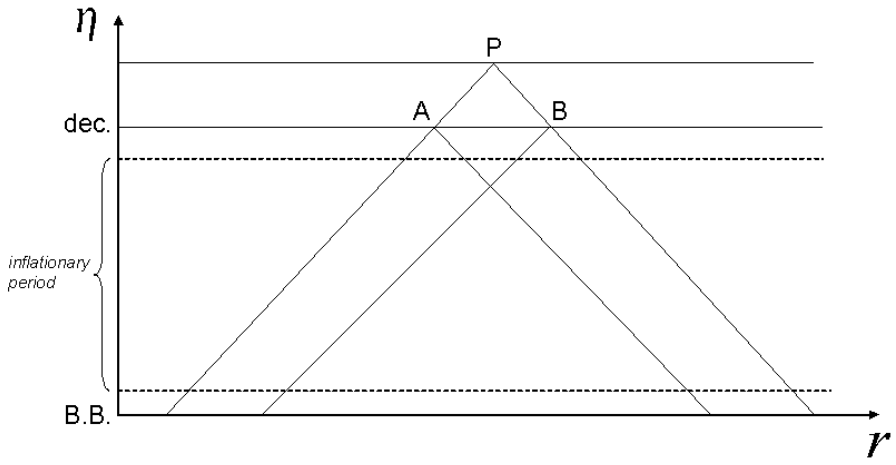


Figure 2.5. Having an exponential expansion for an interval $\Delta t_{\rm inf}$ instead of a radiation driven one ($a(t) \propto t^{1/2}$), causes a dilation $\sim \exp(H\Delta t_{\rm inf})$ in conformal time $\Delta\eta = \int \frac{cdt}{a(t)}$, pushing Big Bang line further into the past in terms of η.

2.6. Measuring the Universe

The two observables for an astrophysical object are its redshift and its apparent brightness. Objects of known actual luminosity are called "standard candles" together with their observed brightness we can define luminosity distance, a key concept in astrophysics and cosmology;

$$d_L^2 \equiv \frac{L}{4\pi I}, \tag{2.22}$$

where L is the actual luminosity (radiative power in the observed wavelength band) and I is the observed intensity. In other words, d_L is the distance an object of luminosity L would be judged to be in static flat space, if it produced an intensity I on Earth.

Characteristics of expansion are determined through an inspection of a set of luminosity distances as a function of redshift values.

Let us consider having a source of light at $t = t_1$ and $r = r_1$ and a receiver at $t = t_0$ and $r = 0$ in spherical coordinates. The spacetime is governed by FRW metric. For the propagation of light we study radial null geodesic, meaning $ds^2 = 0$, $d\theta = 0$,

$d\phi = 0$. We get

$$c^2 dt^2 = a^2(t) \frac{dr^2}{1 - kr^2}, \tag{2.23}$$

and

$$\frac{cdt}{a(t)} = \pm \frac{dr}{(1 - kr^2)^{1/2}}. \tag{2.24}$$

Integrating both sides we find,

$$c \int_{t_1}^{t_0} \frac{dt}{a(t)} = - \int_{r_1}^{0} \frac{dr}{(1 - kr^2)^{1/2}} = f(r_1), \tag{2.25}$$

where $f(r_1)$ depends on curvature parameter k.

Assuming that another light beam is generated at a later time $t = t_1 + dt_1$ and it is observed at $t = t_0 + dt_0$, our equations become,

$$c \int_{t_1 + dt_1}^{t_0 + dt_0} \frac{dt}{a(t)} = - \int_{r_1}^{0} \frac{dr}{(1 - kr^2)^{1/2}} = f(r_1), \tag{2.26}$$

from which we can conclude that,

$$\int_{t_1}^{t_0} \frac{dt}{a} = \int_{t_1 + dt_1}^{t_0 + dt_0} \frac{dt}{a}, \tag{2.27}$$

or simply,

$$\frac{dt_0}{a(t_0)} = \frac{dt_1}{a(t_1)}. \tag{2.28}$$

So we can easily define the cosmological redshift z as a fraction of time intervals or basically frequencies;

$$\frac{dt_0}{dt_1} = \frac{a(t_0)}{a(t_1)} = 1 + z. \tag{2.29}$$

Now let's get back to definition of luminosity distance (2.22). For a static and flat geometry d_L^2 should have the form

$$d_L^2 = a^2(t_0) r_1^2 \tag{2.30}$$

from the line element for the sphere centred at the observer ($dt = dr = 0, t = t_0, r = r_1$),

$$ds^2 = a^2(t_0) r_1^2 (d\theta^2 + \sin^2\theta d\phi^2). \tag{2.31}$$

But in an expanding universe luminosity is reduced by a factor of $(1+z)^2$ since it is energy radiated per unit time and both energy and inverse time interval are redshifted by $(1+z)$. So,

$$d_L^2 = a^2(t_0) r_1^2 (1+z)^2. \tag{2.32}$$

For three available k values Equation 2.25 becomes

$$f(r_1) = c\int_{t_1}^{t_0} \frac{dt}{a} = \begin{cases} \sin^{-1}(r_1), & k = 1 \\ r_1, & k = 0 \\ \sinh^{-1}(r_1), & k = -1 \end{cases} \tag{2.33}$$

To replace dt we take the derivative of (2.29);

$$\frac{dz}{dt} = -(1+z)H(z). \tag{2.34}$$

just to get r_1 in terms of z and Hubble parameter;

$$c\int_{t_1}^{t_0} \frac{dt}{a} = -c\int_{z}^{0} \frac{dz'}{a(1+z')H(z')} = \frac{c}{a(t_0)}\int_0^z \frac{dz'}{H(z')} = f(r_1), \tag{2.35}$$

or

$$r_1 = f^{-1}\left(\frac{c\int_0^z \frac{dz'}{H(z')}}{a(t_0)}\right). \tag{2.36}$$

So luminosity distance from (2.32) becomes,

$$d_L(z) = (1+z)a(t_0)f^{-1}\left(\frac{c\int_0^z \frac{dz'}{H(z')}}{a(t_0)}\right), \tag{2.37}$$

from which follows that scale factor $a(t)$ can be arbitrarily scaled only for flat geometry. We can comment on that result. In curved spacetime scale factor shows up as a characteristic length scale. For example if $k = 1$ any separation calculated from FRW metric has the form,

$$s = a(t)\sin^{-1}(r), \tag{2.38}$$

which means there is a maximum; $r_{\max} = 1$ and $s_{\max} = \frac{\pi}{2}a(t)$. So scale factor entering the calculation of luminosity distance may not be any arbitrary length scale; it is the "diameter of the universe".

For small z, since $f(r) \to r$, expansion of (2.37) gives,

$$d_L \simeq \frac{cz}{H_0}, \tag{2.39}$$

original form of Hubble's law. In other words Hubble's law is small z approximation of this relation.

The expression (2.37) for $d_L(z)$ can be used to test cosmological models. A cosmological model will predict a certain function for $a(t)$, from which $t(z)$ can be in principle found by solving $\frac{a(t)}{a_0} = \frac{1}{1+z}$. Then this can be used to find $H(z)$ via Equation 2.9, finally giving a $d_L(z)$-curve which can be compared against observations.

For flat geometry, both (2.37), the expression for luminosity distance and (2.11) simplify; in fact, we can skip the step of specifying $a(t)$. Luminosity distance becomes

$$d_L(z) = (1+z)c\int_0^z \frac{dz'}{H(z')}. \qquad [\text{for } k=0] \tag{2.40}$$

Since Equation 2.16 is valid for each component of the cosmological fluid, the total energy density is

$$\rho = \sum_i \rho_i^{(0)}(a/a_0)^{-3(1+w_i)} = \sum_i \rho_i^{(0)}(1+z)^{3(1+w_i)}, \tag{2.41}$$

giving us

$$H^2 = {H_0}^2 \sum_i \Omega_i (1+z)^{3(1+w_i)}, \qquad [\text{for } k=0] \tag{2.42}$$

and finally for luminosity distance,

$$d_L(z) = \frac{z+1}{H_0} c\int_0^z \frac{dz'}{\sqrt{\sum_i \Omega_i (1+z')^{3(1+w_i)}}}, \qquad [\text{for } k=0] \tag{2.43}$$

where $\sum_i \Omega_i = 1$.

Now one can make plots of d_L versus z for different numbers of contributions of different perfect fluids as in Figure 2.6 adopted from [11]. For example for the matter dominated model, one gets $d_L(z) = c\frac{2\sqrt{z+1}}{H_0}(\sqrt{z+1}-1)$ whereas for Λ-dominated model, one gets $d_L(z) = c\frac{z(z+1)}{H_0}$. These results correspond to curves a and d respectively in Figure 2.6.

Using (2.37) we may also make analysis of $d_L(z)$ for models other than $k=0$. For example for $k=1$ we have

$$d_L(z) = (1+z)a_0 \sin\left(\frac{c\int_0^z \frac{dz'}{H(z')}}{a_0}\right). \tag{2.44}$$

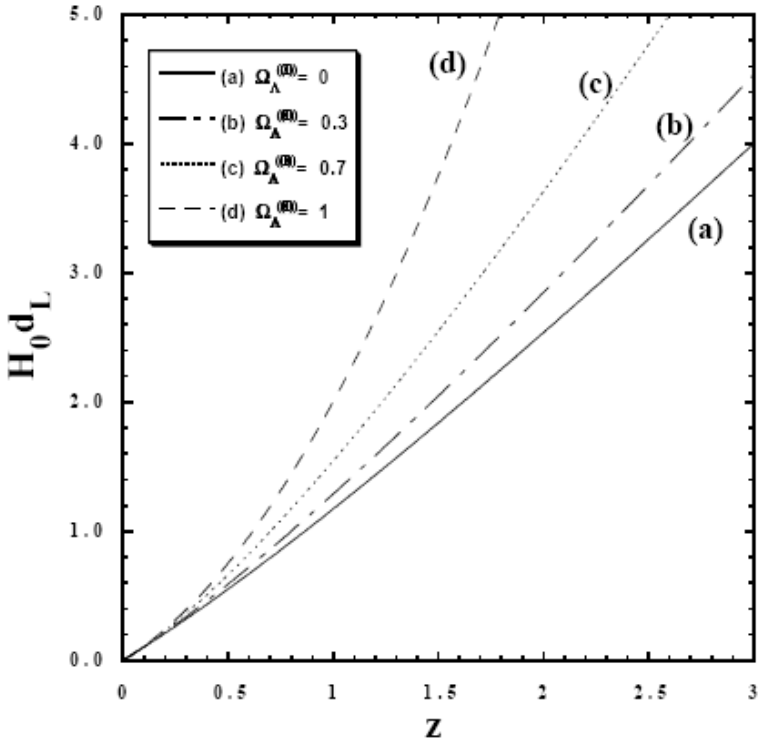


Figure 2.6. Plots showing the expansion characteristics for different amounts of contribution in a "Λ - Cold Dark Matter" two-fluid model (adopted from [11]).

In the matter dominated case [1, Page 734]

$$t(\eta) = \frac{1}{2c} a_{\max}(\eta - \sin(\eta)), \tag{2.45}$$

and

$$a(\eta) = \frac{1}{2} a_{\max}(1 - \cos(\eta)). \tag{2.46}$$

So from definitions it is straightforward to find that

$$H = \frac{c \sin(\eta)}{(1 - \cos\eta) a(\eta)}, \tag{2.47}$$

and

$$\frac{dz}{d\eta} = -\frac{a_0 a_{\max}}{2a^2(\eta)} \sin\eta, \tag{2.48}$$

and replace them in (2.44), which simplifies to

$$d_L = (1+z) a_0 \sin(\eta_0 - \eta). \tag{2.49}$$

Using trigonometric identities "$\sin^2 x + \cos^2 x = 1$" and "$\sin(a-b) = \sin a \cos b - \cos a \sin b$" we may find luminosity distance as a function of redshift as intended;

$$d_L(z) = 2a_0 \sqrt{\frac{a_0}{a_{\max}}} \left[(1 + z - 2\frac{a_0}{a_{\max}}) \sqrt{1 - \frac{a_0}{a_{\max}}} - (1 - 2\frac{a_0}{a_{\max}}) \sqrt{1 + z - \frac{a_0}{a_{\max}}} \right] \tag{2.50}$$

It is worth noting that this results contains two parameters; "a_0 " and "$\frac{a_0}{a_{\max}}$" as opposed to the matter- or Λ-dominated models in the $k = 0$ case, which depend only on the Hubble parameter H_0.

3. RECENT OBSERVATIONS

3.1. Flatness of the Universe

As discussed in Chapter 1, CBR[2] was discovered in 1964 [5]. It has a thermal (blackbody) spectrum at $\sim$ 3K which was predicted to be leftover from the big bang. In 1970 it was pointed out that there should be some temperature fluctuations in CBR due to the inhomogeneities in the photon-baryon plasma in the early pre-combination universe [12, 13, 14]. COBE (Cosmic Background Explorer) satellite confirmed the thermal nature of CBR and recorded the CBR temperature over all the sky, making analysis of temperature fluctuations possible. The largest effect observable was due to "dipole anisotropy"; Doppler shift arising from the velocity of solar system with respect to "the cosmic rest frame"[4] (Figure 3.1). To see the real fluctuations in temperature,

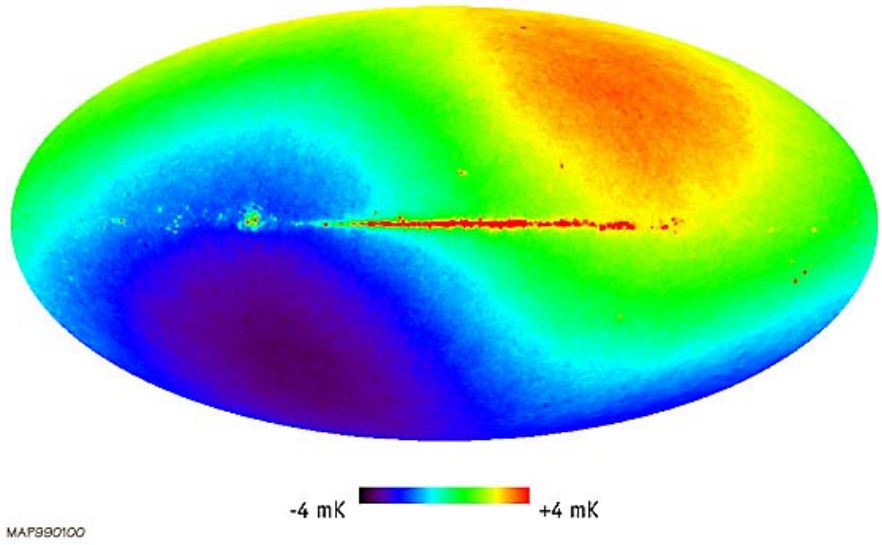


Figure 3.1. Dipole anisotropy based on 4-year mission of COBE. Image is published by COBE Science Working Group.

this dipole term must be subtracted. After the subtraction, COBE data revealed temperature anisotropy of the order 10^{-5} in the CBR due to fluctuations in early universe [15] and its results were later improved by Boomerang [16, 17] and Maxima

[4]This is the frame in which CBR is isotropic to the first approximation. While the existence of a "cosmic rest frame" at first glance seems to be against the tenets of special relativity, obviously CBR can be isotropic only in one frame and the presence of an orderly moving "cosmic fluid" fixes this frame.

[18] experiments and most recently WMAP(Wilkinson Microwave Anisotropy Probe). The WMAP picture of the sky with a resolution down to 0.2 degrees in angular scales is shown in Figure 3.2.

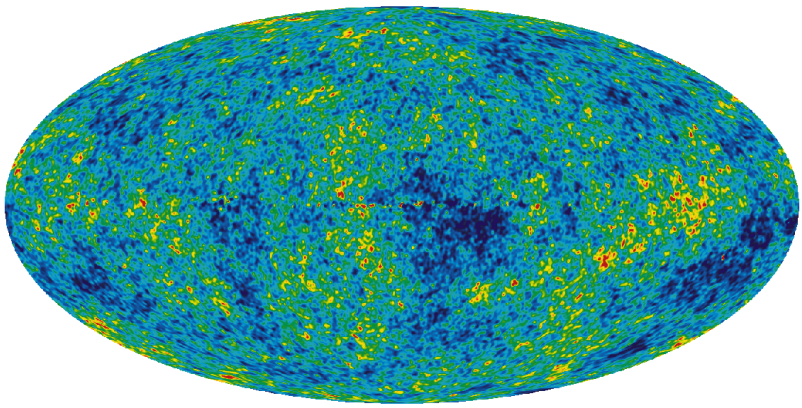


Figure 3.2. WMAP5 picture of CBR showing temperature fluctuations with a resolution of 10^{-4}K. Darkest regions are coldest ones. Image is published by WMAP Science Team.

Analysis of anisotropy of CBR is a useful tool in determining the curvature of the universe. Compression-expansion due to the competing gravitation and radiation-pressure in the photon-baryon fluid created acoustic waves which remain as the temperature fluctuations in the CBR after the last scattering. It is possible to estimate the acoustic horizon –characteristic length of a standing wave– theoretically [19, Page 142]. Propagation of pressure waves in the plasma depends on the velocity of sound v_s in that medium and size of the acoustic horizon is v_s/c times the optical horizon distance, so one should calculate the optical horizon at the time of decoupling first. The horizon distance –part of the universe casually connected– is given by

$$d_H(t) = a(t) \int^t \frac{cdt'}{a(t')}. \tag{3.1}$$

Remembering $a(t) \propto t^{1/2}$ at radiation dominated era one finds that

$$d_H(t_{\rm dec}) = 2ct_{\rm dec}. \tag{3.2}$$

Velocity of sound for radiation epoch is

$$c\left(\frac{\partial p}{\partial \rho}\right)^{1/2} = v_s = c/\sqrt{3}. \tag{3.3}$$

So the acoustic horizon at the time of decoupling may be given as

$$d_{\rm acoustic} = \frac{2}{\sqrt{3}} ct_{\rm dec}. \tag{3.4}$$

But we are searching for these scales in today's sky, so they must be expanded by $(1 + z_{\rm dec})$. They are carried by CBR from the time of decoupling to now, which means the angle they subtend in our sky may be estimated as

$$\theta_{\rm acoustic} \sim \frac{2ct_{\rm dec}(1 + z_{\rm dec})}{\sqrt{3}c(t_0 - t_{\rm dec})} \sim 1^\circ \tag{3.5}$$

where $t_0 = 1.4 \times 10^{10}$ yr, $t_{\rm dec} = 3 \times 10^5$ yr and $z_{\rm dec} = 1100$.

This is our final result and corresponds to the first peak in angular power spectrum vs multipole moment $l \sim \frac{1}{\theta}$ plot (Figure 3.3). But, in a positively curved space the angular size of an oscillating region will be observed bigger than our estimation, whereas in a negatively curved space it will be smaller (Figure 3.4).

The comment on power spectrum graph on WMAP website is an instructive one: "This graph illustrates how much the temperature fluctuates on different angular sizes in the map. Very large angles are on the left, and smaller angles are on the right. Note that there is a large first peak, illustrating a preferred spot size in the map. This means that there is a preferred length for the sound waves in the early universe, just as a guitar string length produces a specific note. The second and third peaks are the

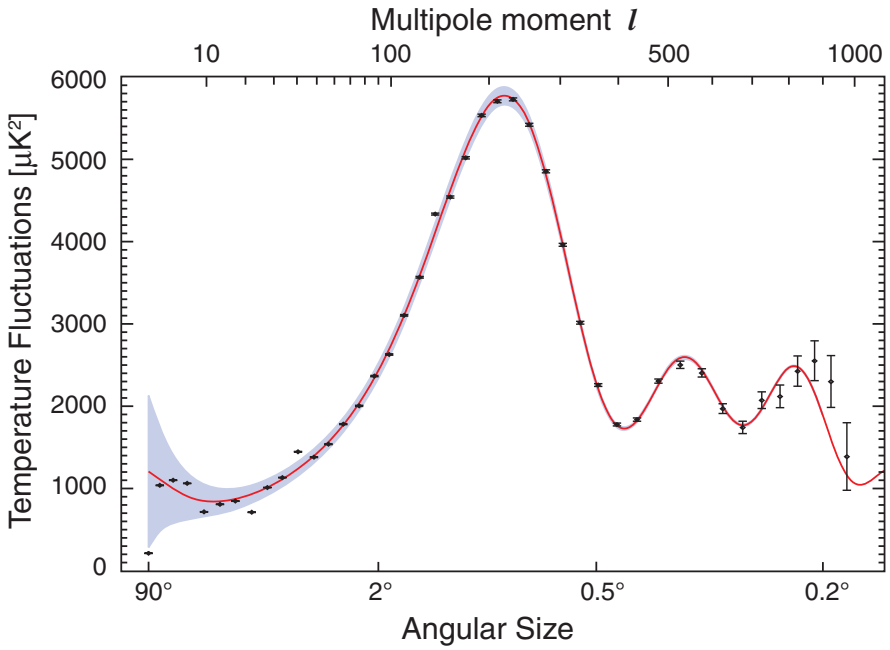


Figure 3.3. Angular power spectrum analysis of WMAP5 data. Image is published by WMAP Science Team.

harmonic overtones of the first peak. The third overtone is now clearly captured in the new 5-year WMAP data. It helps provide evidence for neutrinos." [20]

Position of the first peak in power spectrum of CBR declares a flat universe, in accordance with the idea of inflation. But this also means that the total energy density is equal to critical value. However baryonic matter density is way below this; one or more dark components seem to be dominant in the energy density.

3.2. Accelerated Expansion and Dark Energy

In a matter-dominated universe it is expected to observe a deceleration in expansion. To observe this deceleration we should look deeper into the space. However such observations revealed to us that our universe is an accelerating one and therefore its content may go beyond ordinary matter.

First observational data which indicate an accelerating universe were published in 1998 by "High-z Supernova Team" [21] an international group of astronomers and in 1999 by "Supernova Cosmology Project" (SCP) [22] at Lawrence Berkeley National

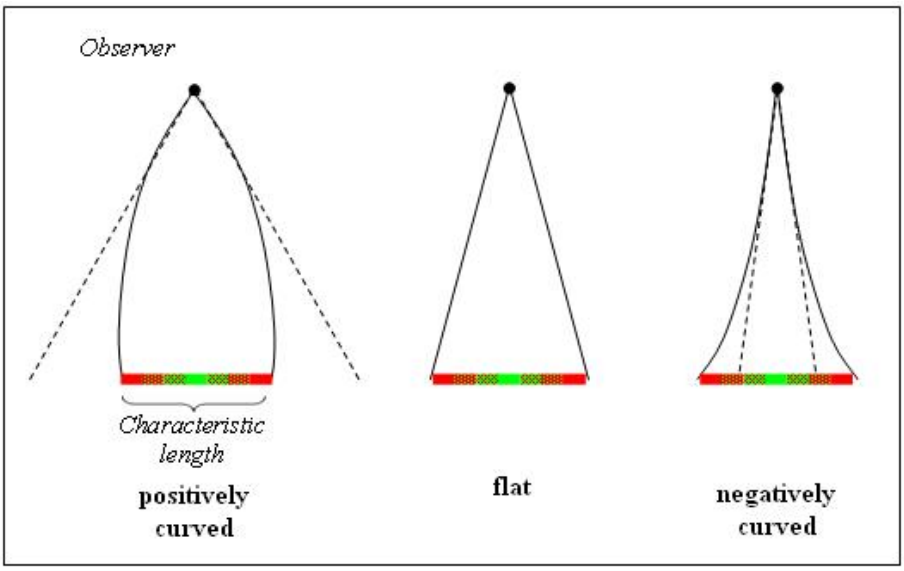


Figure 3.4. Angular size of the observed region depending on curvature.

Laboratory. Using type Ia supernovae as the standard candles, they basically plotted observed brightness of different SNe Ia against their redshifts, in other words, investigated the luminosity distance function $d_L(z)$. With increasing redshift values the data showed an inconsistency with the flat, matter dominated universe ($\Omega = 1$) since the supernovae were observed to be fainter than expected.

That this faintness is evidence for acceleration can be roughly seen by considering Figure 3.5. By Equation 2.29, the z-measurement determines the scale factor $a(t)$ at the time of emission. The fainter the sources are observed, the larger distance they are, meaning the emission times are pushed the further into the past (t_I, t_{II}, t_{III} in Figure 3.5). This gives $a(t)$ curves with less and less deceleration, and if the sources are observed to be faint enough, acceleration.

Of course, for the actual analysis, we must consider the $d_L(z)$ data and see which cosmological model they fit better. The SCP data and theoretical $d_L(z)$ curves, calculated according to Equation 2.37 as derived in Section 2.6 are shown in Figure 3.6. It is easily seen that the data for $z \sim 0.5$ deviate from the $\Omega = 1$, $\Lambda = 0$ model which gained prominence in the last two decades of the 20^{th} century (the curve marked (1,0) in the Figure 3.6). This was a deviation which was undetectable for lower redshift supernova observations in the past.

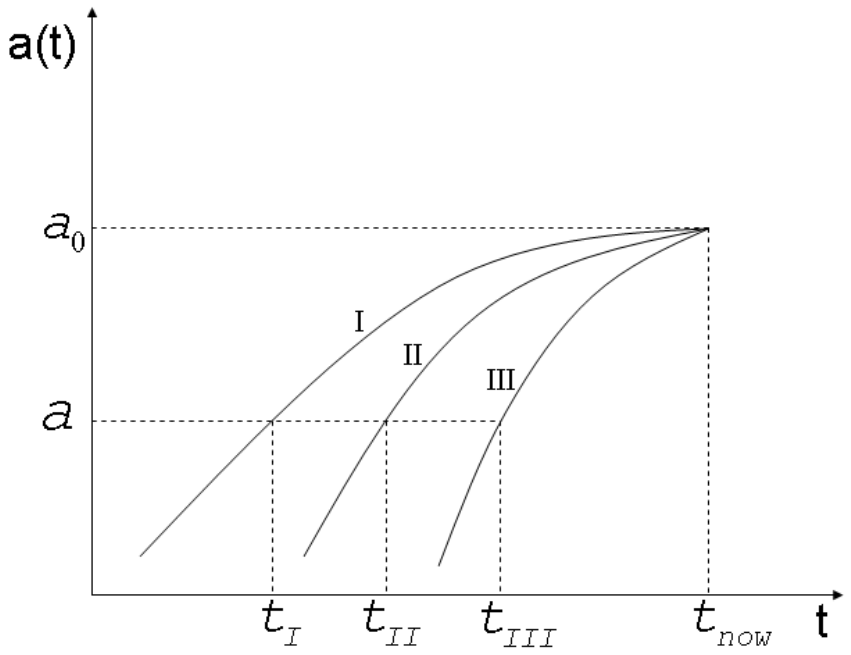


Figure 3.5. Too faint SNe Ia means expansion of the universe is accelerating

In fact, the supernovae were observed to be even fainter than would be predicted for an empty universe (the curve marked (0,0) in Figure 3.6), which for $\Lambda = 0$ would give $\dot{a} = c$ and $\ddot{a} = 0$ (see Equation 2.11 and 2.12). Therefore the data are interpreted as $\ddot{a}$ being positive, i.e. that the universe is accelerating.

Since $a(t)$ is not directly measurable, but H is, one defines the combination

$$q \equiv -\frac{\ddot{a}a}{\dot{a}^2} = -\frac{\dot{H}}{H^2} - 1, \tag{3.6}$$

as the deceleration parameter, which was expected to be positive in the 20^{th} century.

The discovered acceleration (negative q) brings up the possibility of nonzero Λ, also to be discussed in Section 4.1. On Figure 3.6, $d_L(z)$ curves for various values of (Ω_M,Ω_Λ) are shown, where Ω_Λ is defined by

$$\Omega_\Lambda = \frac{\Lambda c^2}{3H^2} \tag{3.7}$$

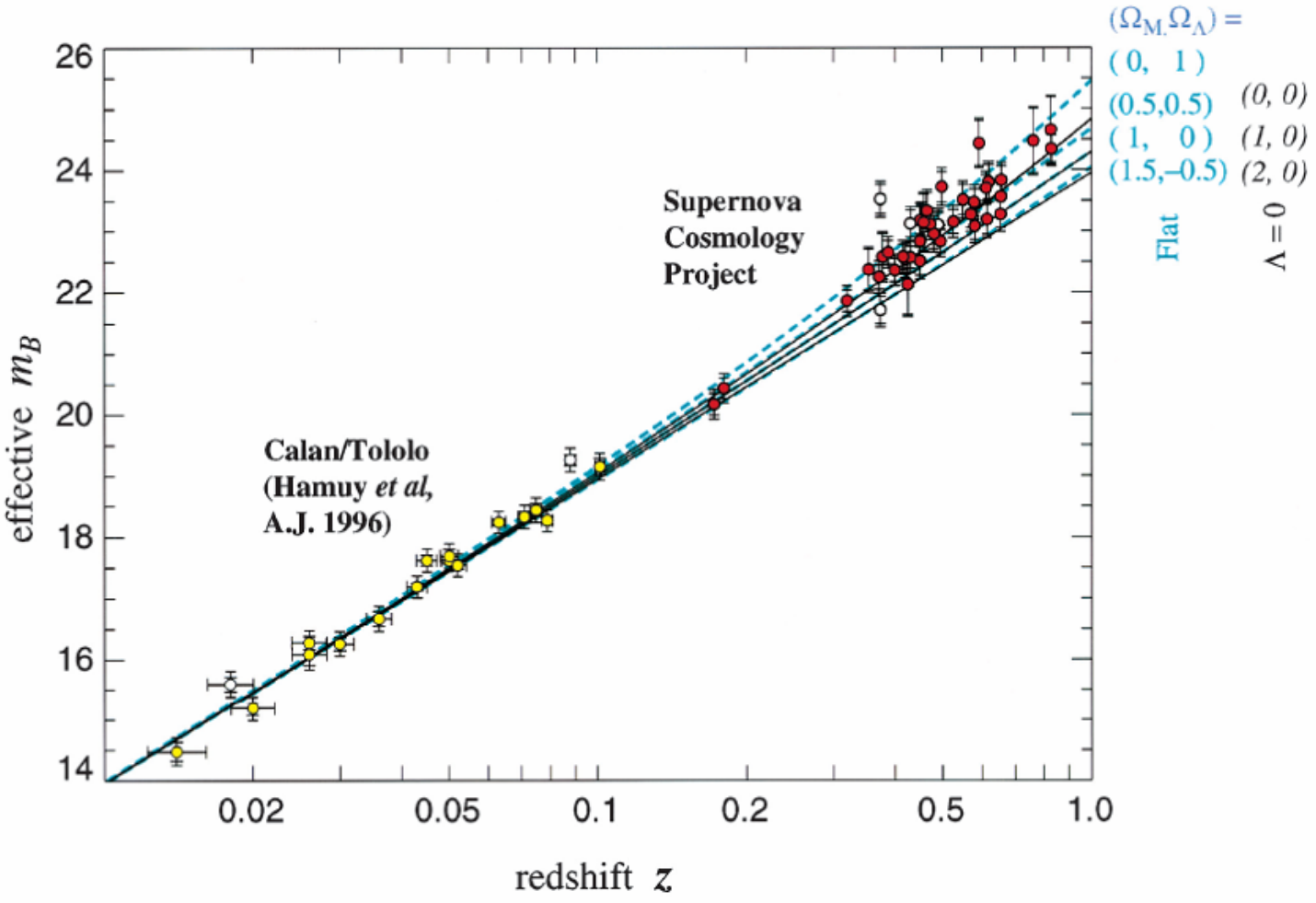


Figure 3.6. Data from Supernova Cosmology Project, together with various theoretical $d_L(z)$-curves (adopted from [22]).

The regions of consistency for SCP data in the Ω_M-Ω_Λ space are shown in Figure 3.7. Since the COBE data tell us that the universe is approximately spatially flat,

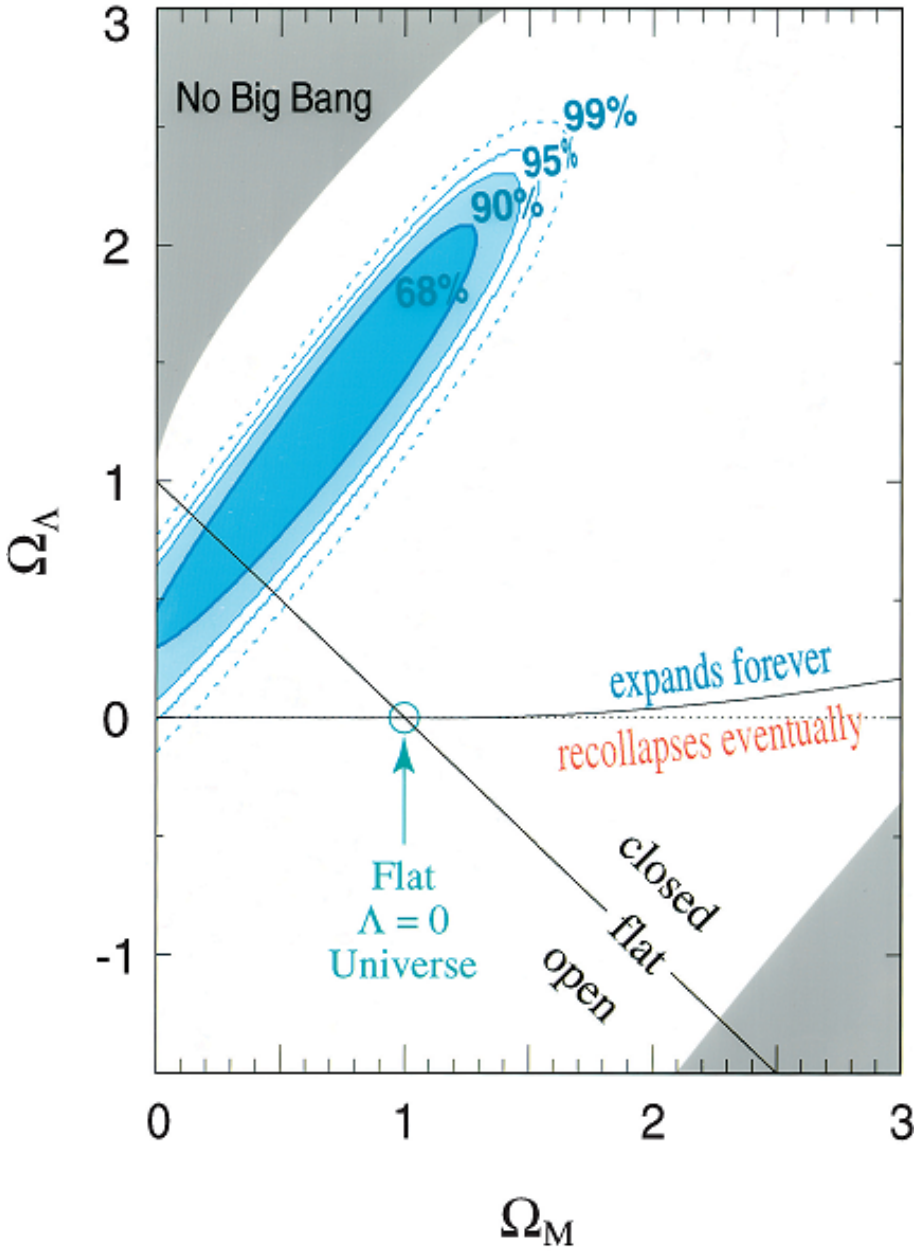


Figure 3.7. Constraints on the energy composition of our universe by the Supernova Cosmology Project (adopted from [22]).

therefore $\Omega_{\text{tot}} \simeq 1$, it is deduced that $\Omega_\Lambda \sim 0.7$ and $\Omega_M \sim 0.3$, as can be seen from the Figure 3.7.

There are two other datasets which came out in the last decade; one is the "Gold data" [23] from the supernovae at $z \geq 1$ detected by *Hubble Space Telescope*, other one is the data from *Supernova Legacy Survey* [24]. The data, together with fits for some (Ω_M, Ω_Λ)-values are shown in Figures 3.8 and 3.9.

To not limit ourselves to explanation by the cosmological constant, we should look for the condition which makes $\ddot{a}(t)$ positive. Extracting $\dot{a}$ from (2.11) and substituting back in (2.12) one can easily show that,

$$\rho + 3p < 0, \tag{3.8}$$

which brings about a condition for the equation of state,

$$p < -\frac{1}{3}\rho. \tag{3.9}$$

To provide the accelerating expansion new source component satisfying the above relation should be introduced. As it seems to be undetectable through any other type of interaction it is "dark", and as its pressure is negative, which is very unusual for matter; it is called "dark energy".

When dark energy is assumed to be (a real or effective) cosmological constant, the above observations conclude that dark energy makes up about the 70% of the content of the universe. Matter, including dark matter, makes up the remaining 30%.

Observations show that Ω for luminous matter is of the order of a few percent, and the Big Bang nucleosynthesis [25, Page 16] calculations give an upper limit of about 0.16 on the Ω of baryonic matter. (The difference between baryonic and luminous Ω may be baryonic matter that has become invisible, such as black holes, brown dwarfs, Jupiter-like objects, etc.)

Therefore, it seems that 14-30% of the universe is made of an unknown kind of matter, and about 70% of something too strange to even call matter. In the coming chapters, we will review the possible explanations of this source, dark energy.

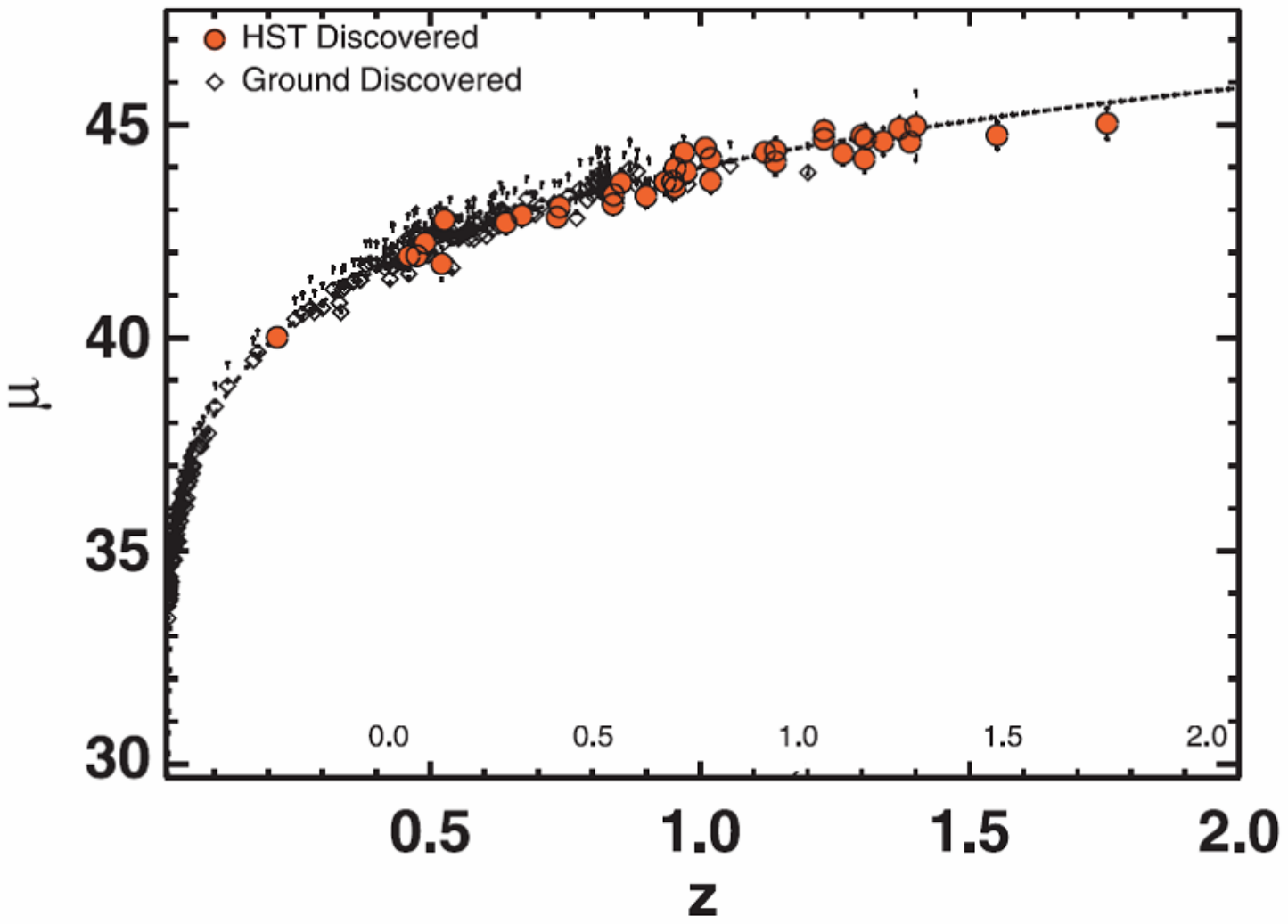


Figure 3.8. "Gold data" plotted over the best fit for a flat cosmology with $\Omega_M = 0.27$ and $\Omega_\Lambda = 0.73$ (adopted from [23]).

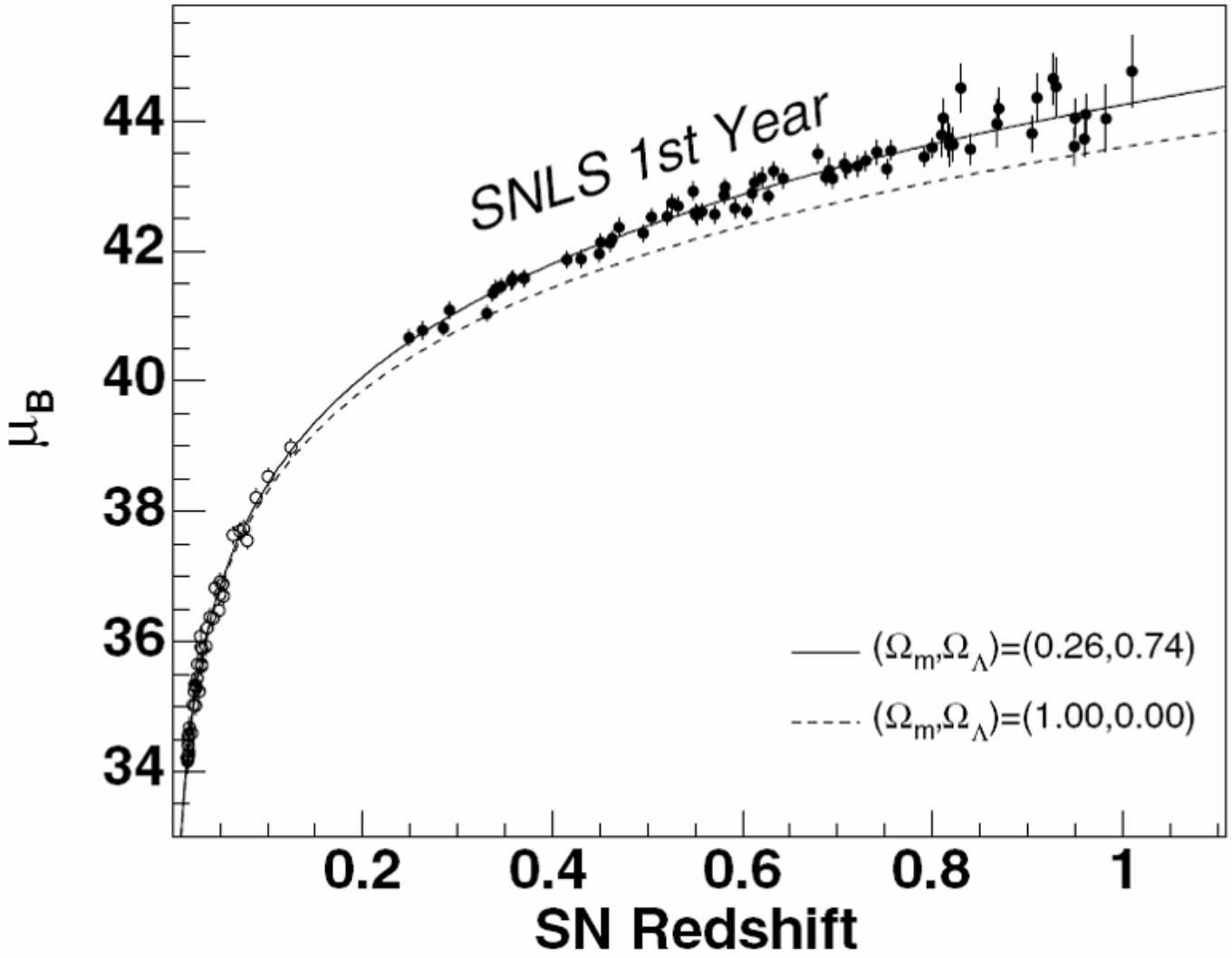


Figure 3.9. First year data from Supernova Legacy Survey with various cosmological models (adopted from [24]).

4. DARK ENERGY CANDIDATES

4.1. Cosmological Constant Revisited

With observations revealing accelerating expansion, the abandoned cosmological constant Λ appeared to be the first explanation that comes to mind since it was repulsive in nature. To ensure acceleration dark energy candidates must produce a repulsion effective over a long-range distance, which cosmological constant does perfectly.

Let us reconsider cosmological Einstein's equations with Λ ; (2.11) and (2.12)

$$\left(\frac{\dot{a}}{a}\right)^2 + \frac{kc^2}{a^2} - \frac{\Lambda c^2}{3} = \left(\frac{8\pi G}{3c^2}\right)\rho,$$

$$2\frac{\ddot{a}}{a} + \left(\frac{\dot{a}}{a}\right)^2 + \frac{kc^2}{a^2} - \Lambda c^2 = -\left(\frac{8\pi G}{c^2}\right)p.$$

The Λ terms in these equations can also be interpreted as describing a perfect fluid with density

$$\rho_\Lambda = \frac{\Lambda c^4}{8\pi G} \tag{4.1}$$

and pressure

$$p_\Lambda = -\frac{\Lambda c^4}{8\pi G}, \tag{4.2}$$

in a cosmological model without a cosmological constant.

Obviously what we came across here is an equation of state with $w = -1$, satisfying the basic condition for DE, Equation 3.9. Named as ΛCDM (Λ-Cold Dark Matter)

this is the simplest and the most traditional model for dark energy and in fact was used as the first interpretation of the new observations (see Figures 3.6-3.9) and is still consistent with all data.

However ΛCDM is subject to doubts arising from particle physics; if interpreted as vacuum energy density, observed value of cosmological constant is 121 orders of magnitude smaller than Planck scale [19, Page 118].

Another downside of the model is that it brings a "cosmic coincidence" into question. It is an observational fact that dark energy and dust-like matter have energy densities of the same order of magnitude today. However, dust energy density changes in time with $1/a(t)^3$, but dark energy density, Λ is constant. This means that acceleration arises as a very recent phenomenon and we live in a special period of universe. To overcome this conundrum dark energy models with time-dependent equation of state are proposed instead of the simple cosmological constant model.

4.2. Quiessence

The term quiessence is attributed to a family of dark energy candidates with constant equation of state, that is, an equation of state of the form (2.15) where w takes a value between -1/3 and -1 [26]. Even though those solutions are mainly ruled out by recent observations they are worth mentioning to present a more complete set of possibilities as some of them have physical interpretations.

Most interesting quiessence models are the ones with $w = -1/3$ and $w = -2/3$ corresponding to cosmic strings and branes respectively [25, Pages 219-228].

4.3. Quintessence

Quintessence is the name of a family of candidates for dark energy corresponding to perfect fluids obeying a dynamical equation of state with w between $-1/3$ and -1. The name can be translated as "fifth element" since it represents a fifth contribution

to energy density of the universe alongside with baryonic matter, radiation, neutrinos and cold dark matter [27]. Of course, it also refers to the ancient concept of the fifth element, which heavenly bodies were supposed to be made of, in contrast to the four elements constituting familiar objects.

Inspired by the inflationary scenarios, quintessence is modelled as a scalar field with some interaction potential $V(\phi)$ minimally coupled to gravity. The Lagrangian for such a scalar field may be given as,

$$L = -\frac{1}{2}g^{\mu\nu}\partial_\mu\phi\partial_\nu\phi - V(\phi) \tag{4.3}$$

Assuming (by the cosmological principle) that the field is uniform in space, we get equation of motion (see Appendix B)

$$\ddot{\phi} + 3H\dot{\phi} + \frac{dV}{d\phi} = 0. \tag{4.4}$$

By varying the Lagrangian with respect to $g^{\mu\nu}$ one gets the energy momentum tensor (see Appendix B)

$$T_{\mu\nu} = \partial_\mu\phi\partial_\nu\phi - g_{\mu\nu}\left[\frac{1}{2}g^{\alpha\beta}\partial_\alpha\phi\partial_\beta\phi + V(\phi)\right]. \tag{4.5}$$

For uniform field, from the $(0-0)$ and $(i-i)$ components of the energy-momentum tensor of this scalar field we can assign the energy density,

$$\rho = \frac{1}{2}\dot{\phi}^2 + V(\phi) \tag{4.6}$$

and pressure,

$$p = \frac{1}{2}\dot{\phi}^2 - V(\phi) \tag{4.7}$$

for an equivalent perfect fluid at rest. Using these assignments in (3.9) we see that

accelerating expansion is only valid for the condition,

$$\dot{\phi}^2 < V(\phi), \tag{4.8}$$

which means that potential giving rise to accelerated expansion must be flat. Also we can easily see that in the $w = -1$ limit $V(\phi)$ is much bigger than $\dot{\phi}^2$ and consequently $\rho \sim V$.

The most important subclass of quintessence is the "tracker" models [28, 29]. In these models dark energy density tracks a path below the radiation density through the radiation-dominated era, and right after the matter-domination its portion in total energy density starts to increase until it tops that of matter (Figure 4.1). These models are proposed to overcome coincidence problem. The most common form is the inverse

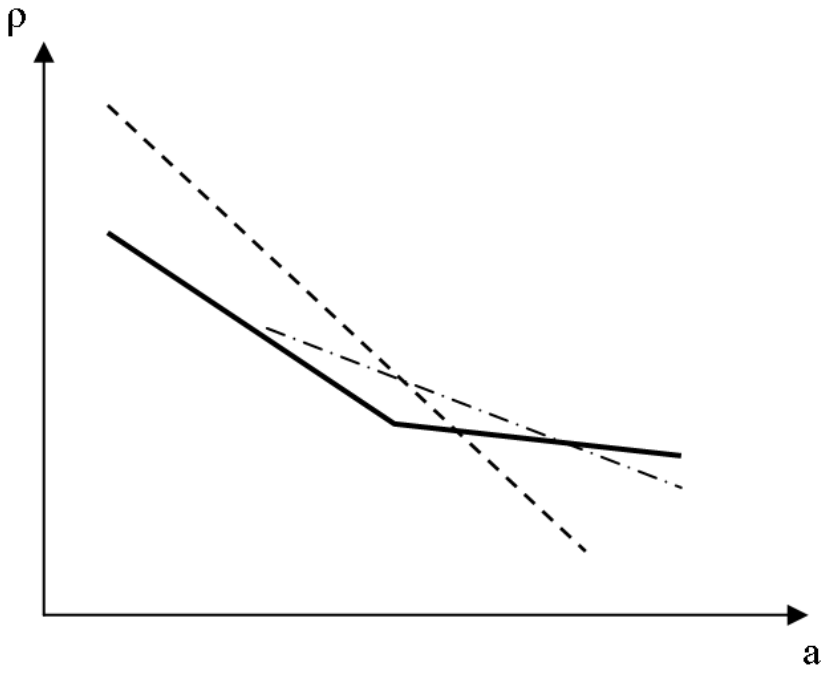


Figure 4.1. "Tracker" quintessence models: Dashed line represents radiation density where dotted-dashed line is matter density. Solid curve is for quintessence "tracker".

power-law potential:

$$V(\phi) = \frac{M^{4+\alpha}}{\phi^{\alpha}}. \tag{4.9}$$

If we solve (4.4) for potential (4.9) in the slow-roll limit ($\ddot{\phi} \approx 0$) for the "background" dominated era (radiation or matter) in a flat universe we get using (2.17),

$$\phi \propto t^{\frac{2}{(\alpha+2)}}. \tag{4.10}$$

Consequently

$$\rho_{\phi} \propto t^{\frac{-2\alpha}{\alpha+2}} \propto a^{\frac{-\alpha 3(w_B+1)}{\alpha+2}}, \tag{4.11}$$

where w_B is the equation of state of the background. On the other hand, (2.16) must also be true for ρ_{ϕ}, giving us

$$w_{\phi} \approx \frac{\frac{\alpha}{2}w_B - 1}{1 + \frac{\alpha}{2}}. \tag{4.12}$$

From above, we can see that w_{ϕ} is always less than w_B, which provides the tracker behaviour; ρ_{ϕ} decays slower than the background, eventually dominating the energy density. Matter-dominated era can not last forever.

Another feature of this potential is that, once the ϕ-field dominates, we can put $w_{\phi} = w_B = w$ in (4.12) and solve to find that w becomes -1, agreeing with actual observations.

4.4. K-essence

It is also proposed that the accelerated expansion of the universe could be driven by non-standard (non-quadratic) kinetic term of a scalar field. Referred to as k-essence ("kinetically driven quintessence") [30], these models are described by a generalized

Lagrangian of the form

$$L = p(\phi, X) \tag{4.13}$$

where

$$X \equiv -\frac{1}{2} g^{\mu\nu} \partial_\mu \phi \partial_\nu \phi, \tag{4.14}$$

together with the condition of the dominance of the kinetic terms.

Variation of this Lagrangian gives [31] (see Appendix B),

$$T_{\mu\nu} = \frac{\partial p(\phi, X)}{\partial X} \partial_\mu \phi \partial_\nu \phi + p(\phi, X) g_{\mu\nu}. \tag{4.15}$$

From above we find that pressure of k-fluid is represented by $p(\phi, X)$ itself and its energy density is (see Appendix B)

$$\rho_\phi = 2X \frac{\partial p}{\partial X} - p. \tag{4.16}$$

It is easily seen that for $p(\phi, X) = X - V(\phi)$, these expressions reduce to (4.6) and (4.7). However, the kinetic-dominance condition means that p is zero near $X = 0$, so we may expand Lagrangian as follows,

$$p(\phi, X) = K(\phi)X + L(\phi)X^2 + \cdots \tag{4.17}$$

We assume that the Lagrangian consists of only these two terms, i.e. contains only $\dot{\phi}^2$ and $\dot{\phi}^4$ terms.[5] Next, we make a field redefinition,

$$d\phi_{\text{new}} = d\phi_{\text{old}} \sqrt{|L/K|}. \tag{4.18}$$

[5] [32] assumes $L > 0$ and eventually that $K < 0$. This is not necessary, and it is possible to proceed as we do, with sign functions.

therefore $X_{\rm new} = |L/K|X_{\rm old}$. Then the pressure of the fluid takes the form,

$$p(\phi, X) = f(\phi)(\text{sign}(K)X + \text{sign}(L)X^2), \tag{4.19}$$

where $\phi \equiv \phi_{\rm new}$, $X \equiv X_{\rm new}$ and $f(\phi) = |K^2(\phi_{\rm old})/L(\phi_{\rm old})|$. So we can find its energy density,

$$\rho_\phi = f(\phi)(\text{sign}(K)X + \text{sign}(L)3X^2), \tag{4.20}$$

and equation of state,

$$w = \frac{1 + \text{sign}(L/K)X}{1 + \text{sign}(L/K)3X}. \tag{4.21}$$

to get negative w, sign(L/K) must be negative. Then the acceleration condition is $1/3 < X < 2/3$.

To find scaling solutions ($w = \text{constant} \Rightarrow \text{X} = \text{constant}$) we should look back at EFE. For a background dominated universe using (2.14) and (2.17) we get [32]

$$\dot{\rho}_\phi = -\frac{2}{t(1 + w_B)}(1 + w_\phi)\rho_\phi \tag{4.22}$$

Solving this equation for ρ_ϕ, recalling $X = \text{constant} \Rightarrow \dot{\phi} = \text{constant}$, we see that

$$f(\phi) \propto \phi^{-\alpha}, \tag{4.23}$$

where

$$\alpha = \frac{2(1 + w_\phi)}{1 + w_B}. \tag{4.24}$$

From this we see that for $\alpha < 2$ we have $w_\phi < w_B$, hence the k-essence can show tracker type behaviour.

4.5. Spintessence

Dark energy may be also a complex scalar field, which is spinning in a $U(1)$-symmetric potential $V(\phi) = V(|\phi|)$. Spintessence is the name given to these class of models [33, 34]. It may be represented as

$$\Phi = \phi(t)e^{i\theta(t)}. \tag{4.25}$$

It is possible to show analytically that this type of field may lead to a late time cosmic acceleration [35]. Varying the relevant Lagrangian (see Appendix B) one gets,

$$\rho_{\rm sp} = \frac{1}{2}(\dot{\phi}^2 + \phi^2\dot{\theta}^2) + V(\phi), \tag{4.26}$$

and

$$p_{\rm sp} = \frac{1}{2}(\dot{\phi}^2 + \phi^2\dot{\theta}^2) - V(\phi). \tag{4.27}$$

So Einstein's equations give,

$$\left(\frac{\dot{a}}{a}\right)^2 = \left(\frac{8\pi G}{3c^2}\right)\left(\rho_M + \frac{1}{2}\dot{\phi}^2 + \frac{1}{2}\phi^2\dot{\theta}^2 + V(\phi)\right), \tag{4.28}$$

and

$$2\left(\frac{\ddot{a}}{a}\right) + \left(\frac{\dot{a}}{a}\right)^2 = \left(\frac{8\pi G}{c^2}\right)\left(-\frac{1}{2}\dot{\phi}^2 - \frac{1}{2}\phi^2\dot{\theta}^2 + V(\phi)\right). \tag{4.29}$$

If we vary the same Lagrangian with respect to ϕ and θ, we get equation of motion for ϕ,

$$\ddot{\phi} + 3H\dot{\phi} - \dot{\theta}^2\phi + V'(\phi) = 0, \tag{4.30}$$

and the conservation law associated with θ,

$$a^3\phi^2\dot{\theta} = A_0. \tag{4.31}$$

For spintessence model described in [34] and [35], $\dot{\theta}$ is considered to be slowly varying, so we are left with,

$$a^3\phi^2 = A. \tag{4.32}$$

Combining (4.28) and (4.29),

$$\frac{\ddot{a}}{a} - \left(\frac{\dot{a}}{a}\right)^2 = \frac{1}{2}\left(\frac{8\pi G}{c^2}\right)\left(-\frac{\rho_0 a_0^3}{2a^3} - \frac{1}{2}\dot{\phi}^2 - \frac{1}{2}\dot{\theta}^2\phi^2\right), \tag{4.33}$$

which can be rearranged by using (4.32) and its derivative,

$$a^3\frac{dH}{dt} = \frac{8\pi G}{c^2}\left(-\frac{1}{2}(\rho_0 a_0^3 + \dot{\theta}^2 A) - \frac{9A}{8}H^2\right), \tag{4.34}$$

and rewritten in a simpler form,

$$\frac{dH}{dx} = -l - mH^2, \tag{4.35}$$

where,

$$\frac{d}{dx} \equiv a^3\frac{d}{dt}. \tag{4.36}$$

To investigate expansion characteristics let us consider the deceleration parameter introduced earlier (3.6)

$$q = -\frac{\dot{H}}{H^2} - 1 = -\frac{H^*}{a^3H^2} - 1, \tag{4.37}$$

where star indicates a derivative with respect to x. So from (4.35),

$$q = -1 + \frac{1}{a^3}\left(\frac{l}{H^2} + m\right). \tag{4.38}$$

We can see that q changes sign at,

$$a_c^3 = \frac{l}{H_c^2} + m. \tag{4.39}$$

Lastly, if we differentiate (4.38),

$$\frac{dq}{da}\Big|_{a=a_c} = -\frac{1}{a_c^4}\left[\frac{l}{H_c^2} + 3m\right], \tag{4.40}$$

it is clearly shown that q is a decreasing at $a = a_c$, so it is possible for the universe to enter an accelerating regime (a negative deceleration parameter) at a definite time in its history if it has a spintessence component.

4.6. Phantom Dark Energy

Observations allow $w < -1$, so one should consider its meaning and consequences. This class of solutions are called "phantom dark energy" [36]. The simplest model can be constructed out of a scalar field with a negative kinetic energy, that is, action

$$S = \int d^4x\sqrt{-g}\left[\frac{1}{2}(g^{\mu\nu}\partial_\mu\phi\partial_\nu\phi)^2 - V(\phi)\right]. \tag{4.41}$$

So we get

$$\rho_{\rm ph} = -\frac{\dot{\phi}^2}{2} + V \tag{4.42}$$

and

$$p_{\rm ph} = -\frac{\dot{\phi}^2}{2} - V. \tag{4.43}$$

For w smaller than -1 one can write,

$$\frac{(-\frac{\dot{\phi}^2}{2} - V)}{(-\frac{\dot{\phi}^2}{2} + V)} = -1 - C, \tag{4.44}$$

where C is an arbitrary positive constant. Relation between V and $\dot{\phi}^2$ is

$$(2 + C)\frac{\dot{\phi}^2}{2} = CV. \tag{4.45}$$

So one may conclude that when $V > \dot{\phi}^2/2$, the scalar field acts as a phanom fluid.

Evolution of the universe dominated by this kind of energy is significantly different from other possible dark energy scenarios. Recall (2.16),

$$\rho \propto a(t)^{-3(1+w)}.$$

For $w < -1$ this means that unlike any other type, phantom energy density grows with expansion. Now integrating (2.11) for flat geometry and solving exactly one gets,

$$a(t) = a(t_m)\left(-w + (1 + w)\frac{t}{t_m}\right)^{\frac{2}{3(1+w)}} \tag{4.46}$$

where t_m is the time the universe ceases to be matter dominated. Above solution is valid for $t > t_m$, when the universe is "phantom" dominated. One can see that in a finite time $t = t_m w/(1 + w)$ and for $w < -1$ scale factor diverges. Every bound object from galaxy clusters to nucleons will be torn apart in the ever increasing phantom field in a finite time and the universe will end up in so-called "Big Rip" singularity [37].

4.7. Chaplygin Gas

Another interesting candidate for dark energy is called "Chaplygin gas" [38], a perfect fluid obeying the equation of state

$$p = -\frac{A}{\rho}, \tag{4.47}$$

where A is constant and positive.

First introduced in aerodynamical context in 1904 [39], Chaplygin gas aroused recent interest of a broader field in physics with its features. It is seen that Chaplygin gas equation of state may be obtained from the Nambu-Goto action in string theory [40], and it is the only fluid admitting a supersymmetric generalization [41].

For the FRW cosmology, from equation 2.13 together with a universe model filled with Chaplygin gas one gets

$$\rho = \sqrt{A + \frac{B}{a^6}}, \tag{4.48}$$

where B is an integration constant. The interesting property of this result is that it asserts a universe dominated by dust-like matter for small values of a

$$\rho \sim \frac{\sqrt{B}}{a^3}, \tag{4.49}$$

where for large values it mimics the empty universe with cosmological constant.

$$\rho \sim \sqrt{A}, \tag{4.50}$$

in other words, displays a transition from matter-domination to cosmological-constant-domination.

4.8. Other Models

There are many other models of dark energy mentioned in literature which are not examined in our work. One of them is *vector field DE* [42]; a vector field replaces the scalar field in quintessence. It is claimed that in this model current cosmological evolution is satisfied without any need for fine-tuning. Some works, which can be summed up under the title *tachyon field DE* [43], are based on tachyon fields which are equivalent to a fluid with an equation state parameter between 0 and -1 while rolling down to their ground state. There are models offering an *oscillating DE* [44] to avoid an eternal acceleration. In these models, the scalar field has a double exponential potential ($V(\phi) = \left(Ae^{a\phi} + Be^{-a\phi}\right)^2$). Lastly, there is *holographic DE* [45] which stems from the holographic principle in quantum gravity; any three-dimensional system can be seen as a two-dimensional information structure encoded on a cosmological horizon. Therefore there is an upper bound on the entropy of that system –our universe in this case– which leads to an upper bound on the energy density [46] ($\rho_\Lambda L^3 < M_{\text{pl}}^2 L$, $L \sim$size of the universe), explaining the extremely small value of vacuum energy.

5. OTHER POSSIBILITIES

5.1. Modified Gravity

Efforts described so far were about defining an energy component causing a late-time acceleration in expansion. They were modifications to stress-energy tensor. However it is also possible to modify left hand side of the EFE; maybe general relativity is just an intermediate step in a more complete theory of gravitation.

One example of such modified models is $f(R)$ gravity. Instead of having the regular Einstein-Hilbert action,

$$S = \frac{1}{2\kappa}\int d^4x\sqrt{-g}R \tag{5.1}$$

a more general form may be proposed,

$$S = \frac{1}{2\kappa}\int d^4x\sqrt{-g}f(R). \tag{5.2}$$

Constructing field equations with this action we get [47]

$$f'(R)R_{\mu\nu} - \frac{1}{2}f(R)g_{\mu\nu} - [\partial_\mu\partial_\nu - g_{\mu\nu}(g^{\alpha\beta}\partial_\alpha\partial_\beta)]f'(R) = \kappa T_{\mu\nu}, \tag{5.3}$$

where a prime denotes a derivative with respect to R. From (0-0) and (i-i) components

$$3H^2 = \frac{\kappa}{f'}\left[\rho + \frac{Rf' - f}{2} - 3H\dot{R}f''\right] \tag{5.4}$$

and

$$2\dot{H} + 3H^2 = -\frac{\kappa}{f'}\left[p + \dot{R}^2 f''' + 2H\dot{R}f'' + \ddot{R}f'' + \frac{1}{2}(f - Rf')\right] \tag{5.5}$$

are found. These can be interpreted as the modified versions of (2.11) and (2.12). The

terms next to ρ and p in parentheses are the effective energy density and pressure of this theory, through which we can assign an effective equation of state with

$$w_{\text{eff}} = \frac{\dot{R}^2 f''' + 2H\dot{R}f'' + \ddot{R}f'' + \frac{1}{2}(f - Rf')}{\frac{Rf'-f}{2} - 3H\dot{R}f''} \tag{5.6}$$

One specific form of $f(R)$ examined in the context of dark energy is [48],

$$f(R) = R - \frac{\mu^{2(n+2)}}{R^n}, \tag{5.7}$$

where μ is a new parameter and n is integer. If we insert this into (5.6) with scale factor evolving as $a \propto t^\alpha$

$$w_{\text{eff}} = -1 - \frac{2n}{3 + 6n - 6\alpha} - \frac{2n}{3\alpha} \tag{5.8}$$

where α is related to dominant energy component as

$$\alpha = \frac{2}{3(w_B + 1)}. \tag{5.9}$$

If the effective term is dominant, equation of state parameter reduces to

$$w_{\text{eff}} = -1 + \frac{2(n+2)}{3(2n+1)(n+1)}. \tag{5.10}$$

For the interval $n = [1, \infty]$ w_{eff} is between $-2/3$ and -1, satisfying the criterion for accelerated expansion without demonstrating phantom behaviour.

5.2. Braneworld Models

Another alternative for dark energy comes from the braneworld theories. In these theories our universe is a 4D "brane" (membrane) embedded in a higher dimensional spacetime (the "bulk") and acceleration is an outcome of this higher dimensional gravity.

DGP (Dvali-Gabadadze-Porrati) model [49] is a popular one defined in a bulk 5D Minkowski space. Let us consider the following action,

$$S = \frac{M_{(5)}^3}{2} \int d^5X \sqrt{|g_{(5)}|} R_{(5)} + \frac{M_{\rm pl}^2}{2} \int d^4x \sqrt{|g|} R, \tag{5.11}$$

where the second term is the regular Einstein-Hilbert action and the first term is its 5D version. $M_{\rm pl}$ is 4D Planck mass and $M_{(5)}$ is 5D Planck mass. The bulk metric $g_{AB}^{(5)}$ induces the 4D metric $g_{\mu\nu}$ as

$$g_{\mu\nu} = g_{AB}^{(5)} \partial_\mu X^A \partial_\nu X^B, \tag{5.12}$$

evaluated at $X^5 = 0$. It is shown that [49] for a characteristic length $r_c = M_{\rm pl}^2 / 2M_{(5)}^3$ gravitational potential changes behaviour. More clearly for $H_0^{-1} < r_c$ potential behaves like $1/r$ resembling Newtonian gravity where for $H_0^{-1} > r_c$ it is like $1/r^2$. This is interpreted as "leakage" of 5D gravity in 4D brane.

Constructing EFE with action (5.11) one gets a modified version of Equation 2.11 (see Appendix C);

$$H^2 + \frac{kc^2}{a^2} = \left(\sqrt{\frac{\rho}{3M_{\rm pl}^2} + \frac{1}{4r_c^2}} + \epsilon \frac{1}{2r_c} \right)^2, \tag{5.13}$$

where $\epsilon = \pm 1$ depending on the sign of $\partial a / \partial X^5$ and k is spatial curvature as usual. Note that Equation 2.11 is recovered for $H \gg 1/r_c$.

Together with (2.14), which still holds on the brane, they are sufficient to know about the cosmology of this model [50]. If one considers the case $k = 0$ and $\epsilon = +1$ in (5.13) it follows that at late times $H \to 1/r_c$ $\rho \to 0$; the universe approaches the de Sitter solution and acceleration without dark energy is possible.

5.3. Backreaction of Cosmological Perturbations

It is also suggested that accelerated expansion isn't there; what we interpret as acceleration is just an observational phenomenon [51]. Observations deduce that acceleration is a recent event, appearing at small redshifts. The most significant property of the universe at small redshifts is large-scale structure formation, so maybe observations which are interpreted as acceleration are due to breakdown of homogeneity and isotropy at late times.

The effect of the inhomogeneity and/or anisotropy on the average expansion rate is called *backreaction*. In an inhomogeneous space different parts with different densities expand at different rates. So volume of the faster growing region increases in fraction and therefore average expansion rate can rise.

To demonstrate how the appearance of acceleration is possible through such a mechanism, let us introduce a toy model consisting of two spherical regions, one overdense and other underdense, with scale factors a_1 and a_2, respectively. Let the underdense region be a void expanding like $a_1 \propto t$ and the overdense region be dust-dominated with $a_2 \propto 1 - \cos\eta$ and $t \propto \eta - \sin\eta$ (see Equations 2.45 and 2.46). η is called the development angle; $\eta = 0$ corresponds to Big Bang singularity and $\eta = \pi$ is where overdense region stops expanding and starts collapsing. Total volume for this model is proportional to

$$a^3 = a_1^3 + a_2^3. \tag{5.14}$$

Hubble and deceleration parameters are

$$H = \frac{\dot{a}}{a} = \frac{a_1^3}{a_1^3 + a_2^3} H_1 + \frac{a_2^3}{a_1^3 + a_2^3} H_2 \equiv v_1 H_1 + v_2 H_2 \tag{5.15}$$

$$q = -\frac{\ddot{a}}{H^2 a} = \frac{H_1^2}{H^2} v_1 q_1 + \frac{H_2^2}{H^2} v_2 q_2 - 2 v_1 v_2 \frac{(H_1 - H_2)^2}{H^2}. \tag{5.16}$$

Hubble parameter is simply the volume-weighted average of H_1 and H_2, but in deceleration expression there is a third term which is non-positive and contributes acceleration.

q is a function of η with one free parameter: fraction of volumes f_1 and $f_2 = 1 - f_1$ at some time throughout the evolution of this model. If we set $f_1 = 0.7$ at $\eta = \pi$, then

$$a_1^3 = \frac{0.7}{\pi^3}(\eta - \sin\eta)^3, \tag{5.17}$$

and

$$a_2^3 = \frac{0.3}{8}(1 - \cos\eta)^3. \tag{5.18}$$

Now we can make a plot of $q(\eta)$ (Figure 5.1).

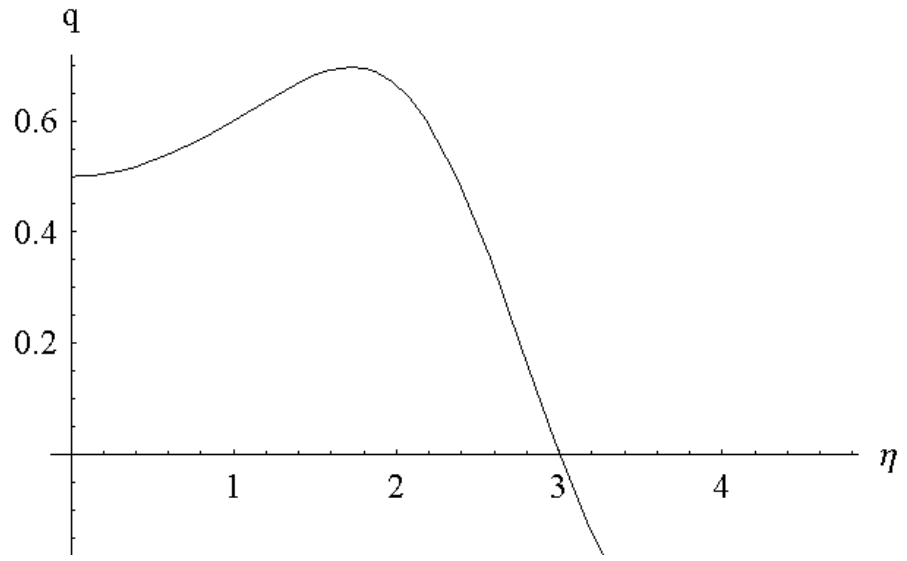


Figure 5.1. It can be clearly seen that model enters a negative deceleration regime.

The physical interpretation of observed acceleration is that fraction of volume of faster expanding regions grow and slower regions are less represented in the average expansion rate.

This toy model is successful in showing that effects of inhomogeneities can mimic acceleration. This constitutes motivation for realistic models and quantitative work.

A similar approach, which also tries to explain acceleration through an inhomogeneous universe, claims that our system is located in the middle of a deep void [52]. In this alternative scenario, FRW metric is replaced by Lemaitre-Tolman-Bondi metric, which presents a radially dependent scale factor, $a(t, r)$. Cosmological principle is set aside and acceleration is again only observational. But it is also claimed that these models are ruled out, because CMB spectrum would be distorted from blackbody [53].

6. COMPARING DARK ENERGY MODELS WITH OBSERVATIONS

6.1. The "Reconstruction" of Dark Energy Properties

One way to test a particular model of dark energy against the observations would be to calculate the function $d_L(z)$ predicted by that model, possibly including a few free parameters. Then, one would find the values of the parameters giving the best fit by some measure (maximum likelihood, χ^2, etc.), and consider the measure of the best fit to be also the measure of the confidence in the model, if the model does not make any other testable predictions.

Another way is to go backward from the data to possible models. In this approach, one "reconstructs" important cosmological functions from the observable ones, in particular, the luminosity distance $d_L(z)$.

For example, (2.40) can be inverted to find $H(z)$ for a flat universe:

$$H(z) = \frac{c}{\frac{d}{dz}\left(\frac{d_L(z)}{1+z}\right)}, \tag{6.1}$$

Then, from (2.11), the dark energy density can be found for late times when radiation is negligible

$$\rho_{\mathrm{DE}} = \frac{3H^2c^2}{8\pi G}(1-\Omega_M), \tag{6.2}$$

where Ω_M is the density of "matter" in terms of critical density.

Similarly, the deceleration parameter becomes

$$q(z) = -\frac{\ddot{a}}{aH^2} = \frac{H'(z)}{H(z)}(z+1) - 1, \tag{6.3}$$

and the dark energy pressure can be found from (2.12) as

$$p_{\mathrm{DE}} = \frac{H^2 c^2}{4\pi G}(q - \frac{1}{2}) \tag{6.4}$$

Dividing p_{DE} by ρ_{DE}, we find the effective equation of state parameter for dark energy.

$$w_{\mathrm{DE}} = \frac{2\left(q - \frac{1}{2}\right)}{3\left(1 - \Omega_M\right)} \tag{6.5}$$

One can then try to see if a certain model predicts an equation of state agreeing with (6.5) or try to construct models that do so.

One can perform this reconstruction by taking $d_L(z)$ to be a function given by its graph drawn from the data after some smoothing procedure. This method, *nonparametric reconstruction*, has the advantage that no preconceptions go into it (except the choice of smoothing procedure), but the numerical differentiations needed in Equation 6.1 for $H(z)$ and Equation 6.5 for w_{DE} will increase the noise coming from the $d_L(z)$ observations.

Alternatively, one can perform *parametric reconstruction* where one takes for one of the functions (e.g. $d_L(z)$) an analytic expression containing some free parameters. Then one can calculate the other functions, and compare models and observations. While this may allow one to handle calculations analytically, it also limits one to the models representable by the initial ansatz.

Examples of reconstruction are shown in Figures 6.1, 6.2 and 6.3.

6.2. Statefinder Diagnostic

The geometry of the universe at a given time t_0 is determined by its scale factor, $a(t_0)$. But for a flat universe, this is not measurable (it can be scaled), and even if our

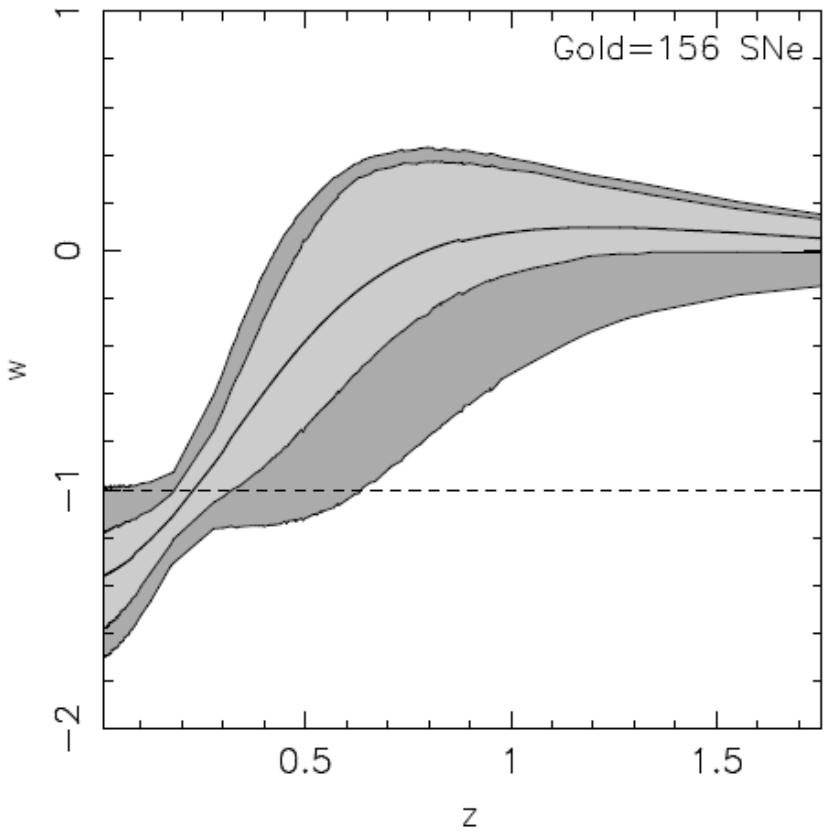


Figure 6.1. Parametric reconstruction of $w(z)$ with an ansatz of the form $H(z) = H_0(\Omega_M(1+z)^3 + A_1 + A_2(1+z) + A_3(1+z)^2)^{(1/2)}$ where $A_1 + A_2 + A_3 = 1 - \Omega_M$. Thick solid line is the best fit ($\Omega_M = 0.3$). 1σ and 2σ confidence levels are given by light grey and dark grey areas (adopted from [54]).

universe is not flat, our scales of observation are much smaller than $a(t_0)$

The time evolution of $a(t)$ means that its time derivatives exist. The measurement of combinations containing these derivatives is of course necessary to increase our understanding of $a(t)$. The combination containing the first derivative, $\frac{\dot{a}}{a}$ is the well-known Hubble parameter, and a dimensionless (unique up to a multiplicative constant) parameter involving the second derivative is also defined, $q = -\frac{\ddot{a}a}{\dot{a}^2} = -\frac{\ddot{a}}{aH^2}$, the deceleration parameter.

The next dimensionless parameter in the sequence is

$$r = \frac{\dddot{a}}{aH^3}, \tag{6.6}$$

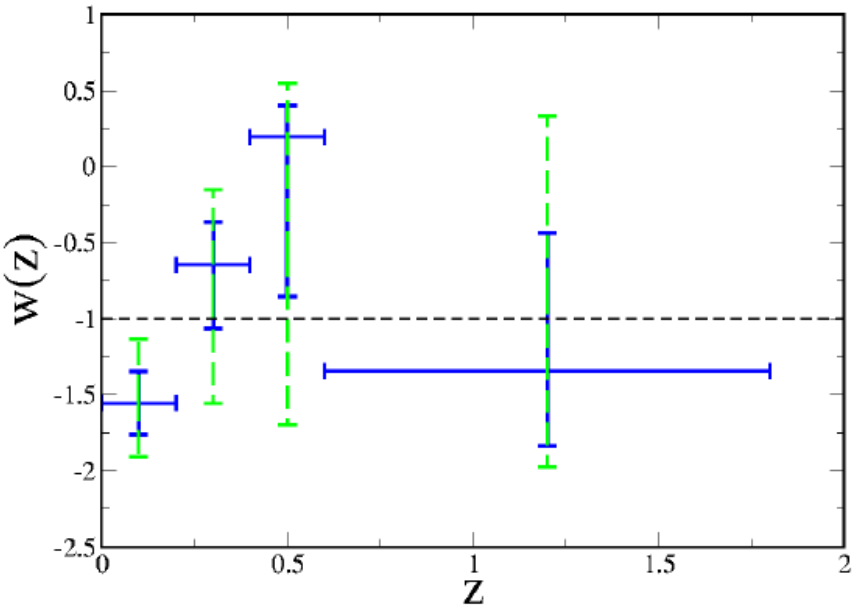


Figure 6.2. Nonparametric reconstruction of $w(z)$. Vertical lines show 1σ and 2σ confidence levels (adopted from [55]).

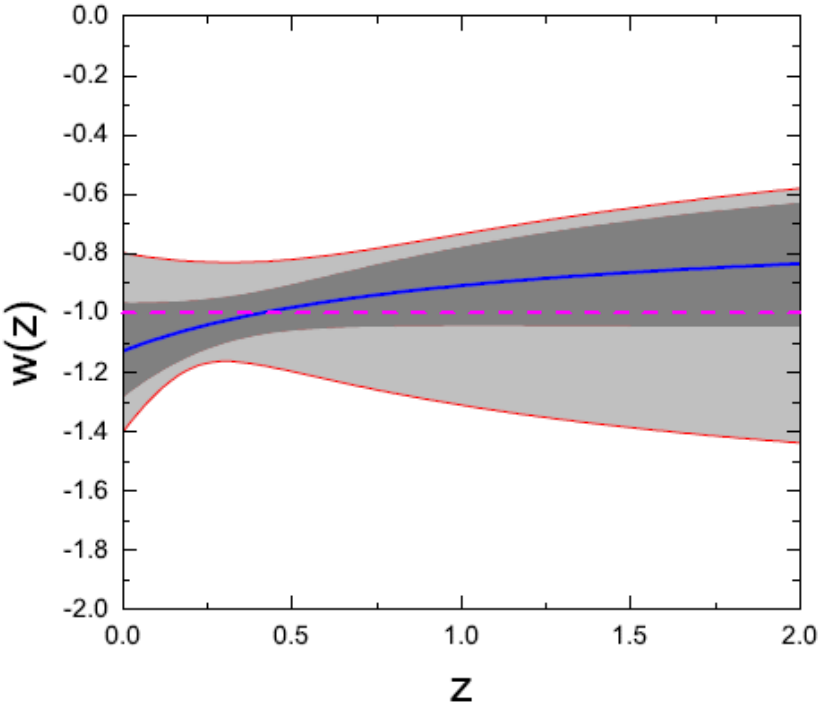


Figure 6.3. Parametric reconstruction of $w(z)$ with an ansatz $w(z) = w_0 + w_1 \frac{z}{1+z}$. Blue line is the best fit ($w_0 = -1.212$, $w_1 = 0.839$) and light grey and dark grey areas represent 68% and 95% confidence levels (adopted from [56]).

It is proposed that the pair $\{r,\, q\}$ can describe a possible universe. Alternatively, the combination

$$s = \frac{r-1}{3(q-1/2)}, \tag{6.7}$$

is defined, and the $\{r,\, s\}$ can be used for the same purpose. r and s are called the *statefinder parameters* [26]. r can be expressed in terms of $H(z)$ (from Equation 6.1) and its derivatives (see Appendix D).

$$r(z) = 1 - \frac{2H'}{H}(1+z) + \left\{ \frac{H''}{H} + \left(\frac{H'}{H}\right)^2 \right\} (1+z)^2, \tag{6.8}$$

and s can also be expressed likewise in terms of observable quantities by using (6.8) and (6.3). Now $r(z)$ and $s(z)$ can be compared with models.

Let us consider the statefinders for a one-fluid cosmological model first (Appendix D):

$$r = 1 + \frac{9}{2}\left(1 + \frac{p}{\rho}\right)\frac{\partial p}{\partial \rho} \tag{6.9}$$

and

$$s = \left(1 + \frac{\rho}{p}\right)\frac{\partial p}{\partial \rho}. \tag{6.10}$$

In the case of cosmological constant where both "p/ρ" and "$\partial p/\partial\rho$" are "-1" (r, s) pair is defined by the fixed point $(1, 0)$, unchanging with time.

For Chaplygin gas (Section 4.8) we get

$$r = 1 + \frac{9}{2}\frac{A}{\rho^2}\left(1 - \frac{A}{\rho^2}\right), \tag{6.11}$$

$$s = \frac{A}{\rho^2} - 1. \tag{6.12}$$

Writing r in terms of s we see that

$$r = 1 - \frac{9}{2} s\,(1+s)\,, \tag{6.13}$$

a parabolic function as shown in the Figure 6.4. The curve starts from the point $(-1, 1)$ where Chaplygin gas mimics matter dominated universe and evolves towards a universe at $(0, 1)$; equivalent to cosmological constant.

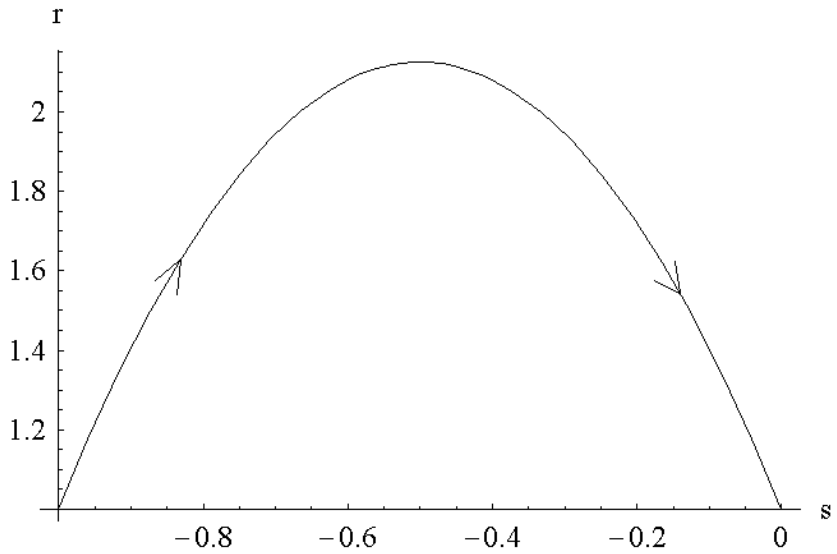


Figure 6.4. r-s evolution of pure Chaplygin universe

Now let us extend our domain of interest by introducing the statefinder parameters for a two-fluid cosmological model. In this case we get (see Appendix D)

$$r = 1 + \frac{9}{2(\rho_1+\rho_2)}\left[\frac{\partial p_1}{\partial \rho_1}(\rho_1+p_1) + \frac{\partial p_2}{\partial \rho_2}(\rho_2+p_2)\right], \tag{6.14}$$

$$s = \frac{1}{(p_1+p_2)}\left[\frac{\partial p_1}{\partial \rho_1}(\rho_1+p_1) + \frac{\partial p_2}{\partial \rho_2}(\rho_2+p_2)\right]. \tag{6.15}$$

If one of the fluids is pressureless dust and the other corresponds to cosmological constant, we see that (r, s) pair is equal to $(1, 0)$ again. This leads us to the interesting result that statefinder pair for universe with cosmological constant is pegged at one specific point unaffected by the presence of dust. Therefore any deviation of the statefinders from this point can be interpreted as a departure from the ΛCDM model.

As for the Chaplygin gas with dust, if we make the necessary substitutions we arrive at the following relation:

$$r = 1 - \frac{9}{2}\frac{s(s+1)}{1+\frac{\rho_m}{\rho_c}}. \tag{6.16}$$

This gives a family of curves shown in Figure 6.5, parametrized by the ratio of energy densities of two fluids. It can be seen that an increase in the dust content results in a lower maximum in evolution curves.

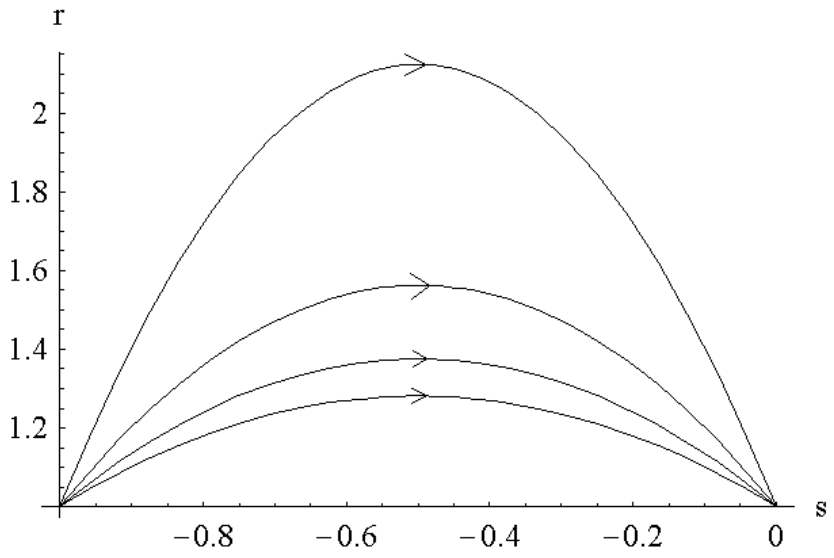


Figure 6.5. r-s evolutions of Chaplygin gas and Dust for different amounts of contribution

Alam *et al.* performed statefinder diagnostic for several dark energy candidates, including quiessence, quintessence, Chaplygin gas and braneworld models [57]. Their results may be summed up in Figures 6.6 and 6.7.

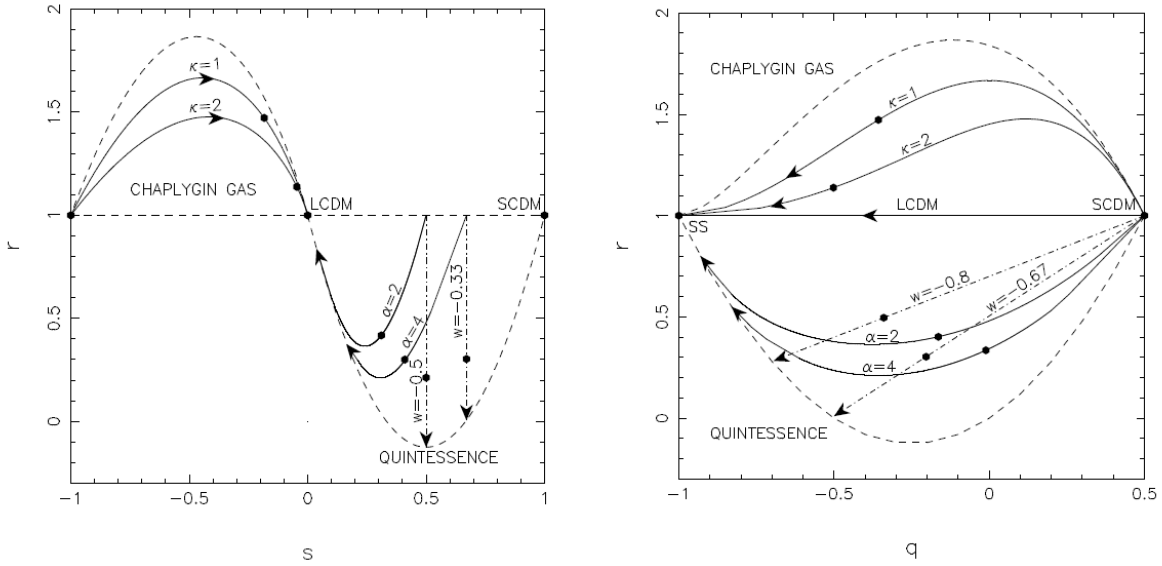


Figure 6.6. Left panel exhibits "r-s" plots for three different dark energy families. Chaplygin gas curves, (upper-left) are identical to ours. On the lower-right we see fluids with constant w (quiessence) with constant $s = 1 + w$ and r going down asymptotically to $1 + \frac{9}{2}w(1 + w)$. Quintessence curves, solid ones on the lower half, are from model described in (4.9). Depending on α, they all have a monotonically decreasing s, where r decreases from unity to a minimum then rises back. Right panel shows same families in a "r-q" diagram (adopted from [57]).

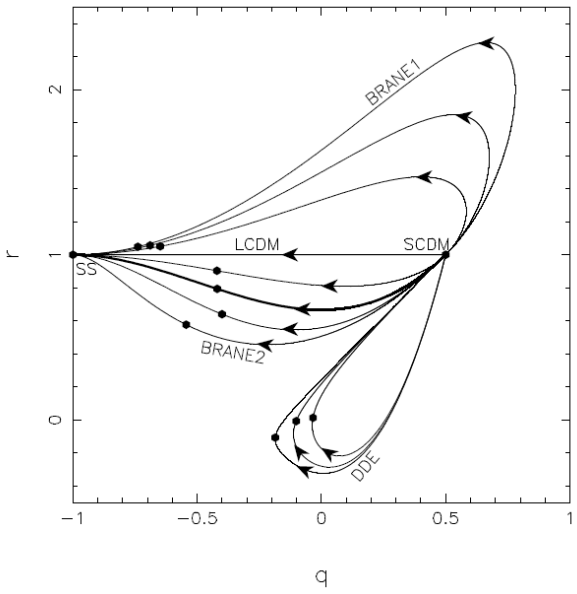


Figure 6.7. Thick solid curve in BRANE2 section is the one we discussed in (5.13) (adopted from [57]).

7. FUTURE OF THE UNIVERSE

Predictions for infinite time evolution requires knowledge of present composition of energy in the universe with future transformations between different kinds and knowledge of present initial conditions for spatial inhomogeneities in the universe [58].

In the second half of the 20^{th} century, when the universe was thought to be matter-dominated, there seemed to be two possibilities for the eventual fate of the universe: Eternal expansion and recollapse ("Big Crunch"). In the Big Crunch, all matter would be broken up by temperature rising to infinity as the universe recollapses; whereas in eternal expansion the universe would be slowly diluted to zero density, matter itself turning over eons into a cold gas of photons and neutrinos due to possible instability of the proton in GUT and due to evaporation of black holes [59]. Speculations were made about the future of intelligence in the eternally expanding "cold death" universe [60]; and cold death-Big Crunch dichotomy led to frequent quoting of Frost.[6]

After the discovery of accelerating expansion, the possibility arose that the future of the universe is dominated by the cosmological constant, eventually ending up in a de Sitter model.

While this model, ΛCDM, is also an eternally expanding "cold death" universe, it also exhibits an event horizon; there exists regions of space in the universe which are forever inaccessible to each other. Alternatively, light from objects which are sufficiently far from an observer will redshift to values undetectable.

Although the matter density reduces practically to zero, it is possible for regions dense enough to preserve their structures. It has been shown that self-binding by local gravity occurs for regions with $\Omega_m > 2.36$ [61], which is several factors less than the

[6] Some say the world will end in fire,
Some say in ice.
From what I've tasted of desire
I hold with those who favor fire.
Robert Frost, "Fire and Ice", *New Hampshire*, 1923.

mean density of the Local Group, including Milky Way and M31 in Andromeda.

The result is island universes isolated from each other by their event horizons. So the universe will be observed to be static and outside of the local island will be empty, removing the necessity to manifest a cosmological principle for the future observers. For them it would be impossible to observe expansion or dark energy, since there won't be any receding distant objects and CBR will vanish due to redshift [62].

The ΛCDM model corresponds to a universe, where the equation of state of the dominant component is $p = -\rho$. For other equations of state, where p/ρ is either a constant less than -1 or not constant, finite-time singularities can arise, the Big Rip mentioned in Section 4.7 being the most popular one. Those singularities are classified according to the behaviour of a, ρ and p [63]:

- Type I (Big Rip) : For $t \to t_s$, $a \to \infty$, $\rho \to \infty$ and $|p| \to \infty$
- Type II : For $t \to t_s$, $a \to a_s$, $\rho \to \rho_s$ and $|p| \to \infty$
- Type III : For $t \to t_s$, $a \to a_s$, $\rho \to \infty$ and $|p| \to \infty$
- Type IV : For $t \to t_s$, $a \to a_s$, $\rho \to 0$ and $|p| \to 0$ and higher derivatives of H diverge.

Values t_s, a_s and ρ_s are constants and a_s and ρ_s are nonzero. Type I, the Big Rip, can be thought of as a more drastic version of the "island universe" scenario above, arising in finite time; and the "islands" are much smaller, to the point of even nuclei being broken apart. Type II is the sudden singularity mentioned in [64]. Type III and IV are mentioned in [65] and [63] respectively and matter density is assumed to be diminished in all of them.

These results are simulated by the equation of state,

$$p = -\rho - f(\rho), \tag{7.1}$$

where $f(\rho)$ presents the deviation from cosmological constant. Putting this into (2.14) and solving for a,

$$a = a_0 \exp\left(\frac{1}{3}\int \frac{d\rho}{f(\rho)}\right). \tag{7.2}$$

From (2.11) with $k = 0$, one may also get an expression for t,

$$t = \int \frac{d\rho}{\kappa\sqrt{3\rho} f(\rho)}. \tag{7.3}$$

Starting with

$$f = A\rho^{\alpha}, \tag{7.4}$$

where A and α are constants. Equations 7.2 and 7.3 become

$$a = a_0 \exp\left[\frac{\rho^{1-\alpha}}{3(1-\alpha)A}\right]. \tag{7.5}$$

$$t = \begin{cases} t_s + \frac{2}{\sqrt{3}\kappa A}\frac{\rho^{-\alpha+1/2}}{1-2\alpha}, & \alpha \neq 1/2 \\ t_s + \frac{\ln(\rho)}{\sqrt{3}\kappa A}, & \alpha = 1/2 \end{cases} \tag{7.6}$$

From these one can deduce that for $\alpha > 1$ there exists type III singularity. For $1/2 < \alpha < 1$ and $A > 0$ we have a type I singularity. If A is negative a goes to 0, corresponding to Big Crunch.

Next we may consider a function of the form,

$$f(\rho) = C(\rho_0 - \rho)^{-\gamma}, \tag{7.7}$$

where C, ρ_0 and γ are constants. Now we have,

$$a = a_0 \exp\left[-\frac{(\rho_0 - \rho)^{\gamma+1}}{3C(\gamma+1)}\right] \tag{7.8}$$

and

$$t \simeq t_s - \frac{(\rho_0 - \rho)^{\gamma+1}}{\kappa C\sqrt{3\rho_0}(\gamma+1)}. \tag{7.9}$$

From above we see that for $\rho = \rho_0$ a is finite and $t = t_s$, hence there exists a type II singularity.

For a type IV singularity one should have a more detailed analysis but it is adequate to mention that it arises for a function of the form

$$f = \frac{AB\rho^{\alpha+\beta}}{A\rho^{\alpha} + B\rho^{\beta}}. \tag{7.10}$$

To summarize, cosmological models advanced since the observation of accelerating expansion have enriched the spectrum of possible futures for the universe, but we still seem to have the two basic possibilities of long, drawn-out death and violent disaster after finite time; only more extreme.

8. CONCLUSIONS AND PROSPECTS

History of cosmology has depended very much on the observations and its future is not going to be any different. On the contrary, inclusion of space-based instruments such as space probes and space observatories carried precision and range of observations to a higher level. First space observatory to perform a survey of entire sky was Infrared Astronomical Satellite (IRAS) which was launched in 1983 by NASA for a ten months mission. It mapped the 96% of the sky at infrared wavelengths.

COBE satellite (Section 3.1) was the next big step. It was regarded as "the starting point for cosmology as a precision science".[7] In accordance with this definition, COBE, with its perfectly fitting data, proved the blackbody nature of CBR, which was a disputed subject due to conflicting and poor data from earth-based experiments.

WMAP, the follow-up to COBE, is launched in 2001. Its five-year data (WMAP5) are released in 2008, which include most precise values on Ω_M and Ω_Λ up to date. Its mission will end in September 2008. By the time of writing of this text Planck satellite –the new anisotropy probe– is launched. Its mission is to measure anisotropy of CBR over the entire sky with a higher angular resolution than WMAP.

For the detailed expansion characteristics of the universe, most reliable data are from SNe Ia observations which we discussed in Section 3.2. Although some of these surveys benefited from Hubble Space Telescope, most of them used earth-based observatories. The data favour ΛCDM model, but theorists present alternatives to it (Chapters 4 and 5) because of the so-called coincidence and fine-tuning problems (Section 4.1). Statefinder diagnostic (Section 6.1) is an example of the fact that to varify or falsify these models we need a wider knowledge of $a(t)$.[8] Once again space-based observatories are in agenda.

[7] Phrase belongs to the Nobel Prize committee.

[8] Expressions $\dddot{a}$ and $\ddddot{a}$, which are used in construction of statefinder parameters, are nothing but third and forth terms in Taylor expansion of $a(t)$.

JDEM (Joint Dark Energy Mission) of NASA is the most promising future research, which is expected to enlighten the dark energy problem. It is going to employ a new space observatory –to be launched in next decade– and make use of several observation techniques such as weak gravitational lensing, baryon acoustic oscillation measurements and once again it is going to examine SNe Ia. At first there were different telescope proposals for JDEM, but by the end of 2008 it was announced that none of them will be selected but the observatory will combine most of the features of the candidates.

To conclude, we reiterate our first paragraph: A revolution in cosmology was unleashed by detailed observations of CBR by COBE and WMAP; and by observations of supernovae at literally cosmological distances by HST and other superb telescopes. These observations not only enriched the set of possible universes, they also transformed cosmology from a discipline of orders-of magnitude to a precision science, as alluded to on the last page. It is an exciting time to do cosmology.

APPENDIX A: MATHEMATICAL DEFINITIONS AND CONVENTIONS

To begin with let us introduce the famous Einstein convention of which we make continuously use,

$$a_i b^i \equiv \sum a_i b_i. \tag{A.1}$$

Next we define the following "connection relations"

$$\Gamma^{\alpha}_{\beta\gamma} \equiv \frac{1}{2} g^{\alpha\mu}(g_{\mu\beta,\gamma} + g_{\mu\alpha,\beta} - g_{\beta\gamma,\mu}), \tag{A.2}$$

where the expression in parantheses is called the Christoffel symbol of the first kind and commas indicate partial derivatives.

Eventually we define Riemann curvature tensor as follows,

$$R^{\alpha}_{\beta\gamma\delta} \equiv \Gamma^{\alpha}_{\beta\delta,\gamma} - \Gamma^{\alpha}_{\beta\gamma,\delta} + \Gamma^{\mu}_{\beta\delta}\Gamma^{\alpha}_{\mu\gamma} - \Gamma^{\mu}_{\beta\gamma}\Gamma^{\alpha}_{\mu\delta}. \tag{A.3}$$

One contraction of Riemann tensor is defined as Ricci tensor by

$$R_{\mu\nu} = R^{\alpha}_{\mu\alpha\nu}, \tag{A.4}$$

and an additional contraction leads to Ricci scalar,

$$R = R^{\alpha}_{\alpha}, \tag{A.5}$$

Now it is suitable to define Einstein tensor,

$$G_{\mu\nu} = R_{\mu\nu} - \frac{1}{2} g_{\mu\nu} R, \tag{A.6}$$

the appropriate linear combination of Ricci tensor and Ricci scalar for the left hand side of the Einstein equations.

APPENDIX B: SCALAR FIELD IN COSMOLOGY

B.1. Quintessence

The Lagrangian for a real scalar field is

$$L = -\frac{1}{2} g^{\mu\nu} \partial_\mu \phi \partial_\nu \phi - V(\phi). \tag{B.1}$$

For a uniform field and the FRW metric this reduces to

$$L = \frac{1}{2} \dot{\phi}^2 - V(\phi). \tag{B.2}$$

To find equation of motion of the field one may vary its action with respect to ϕ or equivalently write down the Euler-Lagrange equation

$$\frac{d}{dt} \left(\frac{\partial}{\partial \dot{\phi}} (\sqrt{-g} L) \right) - \frac{\partial (L\sqrt{-g})}{\partial \phi} = 0, \tag{B.3}$$

so

$$\ddot{\phi} \sqrt{-g} + \dot{\phi} \frac{d(\sqrt{-g})}{dt} + \frac{\partial V}{\partial \phi} \sqrt{-g} = 0, \tag{B.4}$$

where

$$\sqrt{-g} = a^3 \sin\theta \frac{r^2}{\sqrt{1 - kr^2}}. \tag{B.5}$$

Finally we get

$$\ddot{\phi} + 3H\dot{\phi} + \frac{\partial V}{\partial \phi} = 0. \tag{B.6}$$

The energy-momentum tensor is defined as follows [1, Section 21.3]

$$T_{\mu\nu} = -2\frac{\delta L}{\delta g^{\mu\nu}} + g_{\mu\nu}L, \tag{B.7}$$

so

$$T_{\mu\nu} = \partial_\mu\phi\partial_\nu\phi - g_{\mu\nu}\left(\frac{1}{2}g^{\alpha\beta}\partial_\alpha\phi\partial_\beta\phi + V(\phi)\right). \tag{B.8}$$

Energy-momentum tensor of a perfect fluid is

$$T_{\mu\nu} = (\rho + p)u_\mu u_\nu + pg_{\mu\nu}.$$

If we want to identify (B.8) with the $T_{\mu\nu}$ of a perfect fluid at rest (i.e. $u_i = 0$), for a uniform field we find energy density

$$T_{00} = \rho = \frac{1}{2}\dot{\phi}^2 + V(\phi), \tag{B.9}$$

and pressure

$$T_{11} = g_{11}p = g_{11}\left(\frac{1}{2}\dot{\phi}^2 - V(\phi)\right). \tag{B.10}$$

B.2. K-essence

K-essence is described by the Lagrangian

$$L = p(\phi, X), \tag{B.11}$$

where

$$X = -\frac{1}{2}g^{\mu\nu}\partial_\mu\phi\partial_\nu\phi. \tag{B.12}$$

From (B.7)

$$T_{\mu\nu} = -2\frac{\delta p(\phi, X)}{\delta g^{\mu\nu}} + g_{\mu\nu}p(\phi, X), \tag{B.13}$$

where

$$\frac{\partial p}{\partial g^{\mu\nu}} = \frac{\partial p}{\partial X}\frac{\partial X}{\partial g^{\mu\nu}} = -\frac{1}{2}\frac{\partial p}{\partial X}\partial_\mu\phi\partial_\nu\phi. \tag{B.14}$$

So, energy-momentum tensor is given by

$$T_{\mu\nu} = \frac{\partial p}{\partial X}\partial_\mu\phi\partial_\nu\phi + g_{\mu\nu}p, \tag{B.15}$$

from which we get

$$\rho = \frac{\partial p(\phi, X)}{\partial X}\dot{\phi}^2 - p(\phi, X), \tag{B.16}$$

and

$$p = p(\phi, X). \tag{B.17}$$

Also from (B.3) we can find equation of motion for this field

$$\frac{d}{dt}\left(\sqrt{-g}\frac{\partial p}{\partial \dot{\phi}}\right) - \sqrt{-g}\frac{\partial p}{\partial \phi} = 0. \tag{B.18}$$

On the other hand,

$$\frac{\partial p}{\partial \dot{\phi}} = \frac{\partial p}{\partial X}\dot{\phi}, \tag{B.19}$$

so,

$$3H\frac{\partial p}{\partial \dot{\phi}} + \frac{d}{dt}\left(\frac{\partial p}{\partial X}\dot{\phi}\right) - \frac{\partial p}{\partial \phi} = 0. \tag{B.20}$$

we can expand the middle term

$$\frac{d}{dt}\left(\frac{\partial p}{\partial X}\dot{\phi}\right) = \frac{\partial^2 p}{\partial X^2}\frac{\partial X}{\partial t}\dot{\phi} + \frac{\partial p}{\partial X}\ddot{\phi} = \frac{\partial^2 p}{\partial X^2}\dot{\phi}\ddot{\phi}\dot{\phi} + \frac{\partial p}{\partial X}\ddot{\phi}, \tag{B.21}$$

finally getting the equation of motion

$$3H\frac{\partial p}{\partial \dot{\phi}} + \left(\frac{\partial^2 p}{\partial X^2}\dot{\phi}^2 + \frac{\partial p}{\partial X}\right)\ddot{\phi} - \frac{\partial p}{\partial \phi} = 0. \tag{B.22}$$

B.3. Spintessence

For spintessence, one considers a complex scalar field. Then

$$\Phi = \phi(t)e^{i\theta(t)}, \tag{B.23}$$

where $\phi(t)$ and $\theta(t)$ are real. Derivative squared of this field is

$$(\dot{\Phi})^2 = \dot{\Phi}\dot{\Phi}^* = \dot{\phi}^2 + \phi^2\dot{\theta}^2. \tag{B.24}$$

So, from (B.9) and (B.10) we easily find

$$\rho_{\rm sp} = \frac{1}{2}(\dot{\phi}^2 + \phi^2\dot{\theta}^2) + V(\phi), \tag{B.25}$$

and

$$p_{\rm sp} = \frac{1}{2}(\dot{\phi}^2 + \phi^2\dot{\theta}^2) - V(\phi). \tag{B.26}$$

Varying the Lagrangian of this field,

$$L = \frac{1}{2}(\dot{\Phi})^2 - V(\phi). \tag{B.27}$$

we get Euler-Lagrange equation for ϕ

$$\frac{d}{dt}(a^3\dot{\phi}) - a^3(\phi\dot{\theta}^2 - V') = 0, \tag{B.28}$$

from which we get our first equation of motion

$$\ddot{\phi} + 3H\dot{\phi} - \dot{\theta}^2\phi + V'(\phi) = 0. \tag{B.29}$$

If we vary the same Lagrangian for θ we get

$$\frac{d}{dt}(a^3 2\phi^2\dot{\theta}) = 0 \Rightarrow a^3\phi^2\dot{\theta} = A_0. \tag{B.30}$$

APPENDIX C: COSMOLOGY ON A BRANE IN A 5D BULK

The line element for a 5D spacetime in which our 4D universe is embedded is

$$ds^2 = g_{AB}dX^A dX^B = g_{\mu\nu}dx^\mu dx^\nu + b^2 dX^5 dX_5, \tag{C.1}$$

where we have assumed that X^5 is "orthogonal" to our universe. Since our universe is homogeneous, the line element can be written as follows

$$ds^2 = -n^2(\tau, y)d\tau^2 + a^2(\tau, y)\gamma_{ij}dx^i dx^j + b^2(\tau, y)dy^2, \tag{C.2}$$

where $y \equiv X^5$. EFE for this spacetime can be written as

$$R_{AB} - \frac{1}{2}Rg_{AB} = \frac{1}{M^3_{(5)}}(T_{AB} + U_{AB}), \tag{C.3}$$

where U_{AB} is the contribution from scalar curvature of the brane. (0-0) component of the left hand side is [66]

$$G_{00} = 3\left[\frac{\dot{a}}{a}\left(\frac{\dot{a}}{a} + \frac{\dot{b}}{b}\right) - \frac{n^2}{b^2}\left(\frac{a''}{a} + \frac{a'}{a}\left(\frac{a'}{a} - \frac{b'}{b}\right)\right) k\frac{n^2}{a^2}\right], \tag{C.4}$$

and for the energy-momentum tensor we have

$$T^{\text{bulk}}_{00} = -\rho_B, \tag{C.5}$$

$$T^{\text{brane}}_{00} = \frac{\delta(y)}{b}(-\rho_b), \tag{C.6}$$

and

$$U_{00} = -\frac{3\delta(y)}{b} M_{\rm pl}^2 \left(\frac{\dot{a}^2}{a^2} + k\frac{n^2}{a^2} \right). \tag{C.7}$$

First integral of (C.4) gives

$$\frac{(a'a)^2}{b^2} - \frac{(\dot{a}a)}{n^2} - ka^2 + \frac{a^4}{6M_{(5)}^3}\rho_B + C = 0, \tag{C.8}$$

where prime denotes a derivative with respect to y, dot with respect to τ and C is an integration constant. To consider the energy density in the brane ($y = 0$) let us introduce a junction condition

$$\frac{a'}{ab} = -\frac{1}{3M_{(5)}^3}\rho_b + \frac{M_{\rm pl}^2}{M_{(5)}^3 n^2} \left(\frac{\dot{a}^2}{a^2} + k\frac{n^2}{a^2} \right). \tag{C.9}$$

which relates the jumps of the extrinsic curvature across the brane to the energy-momentum tensor inside the brane [67]. If we replace a' in (C.8)

$$\epsilon \sqrt{H^2 - \frac{1}{M_{(5)}^3}\rho_B - \frac{C}{a^4} + \frac{kc^2}{a^2}} = \frac{M_{\rm pl}^2}{2M_{(5)}^3} \left(H^2 + \frac{kc^2}{a^2} \right) - \frac{1}{6M_{(5)}^3}\rho_b \tag{C.10}$$

which can be rewritten ($\rho_B = 0, C = 0$)

$$H^2 + \frac{kc^2}{a^2} = \left(\sqrt{\frac{\rho_b}{3M_{\rm pl}^2} + \frac{1}{4r_c^2}} + \epsilon\frac{1}{2r_c} \right)^2 \tag{C.11}$$

where $r_c = M_{\rm pl}^2/2M_{(5)}^3$.

APPENDIX D: DERIVATIONS REGARDING STATEFINDER PARAMETERS

Second derivative of H gives

$$\ddot{H} = rH^3 + qH^3 - 2H\dot{H}. \tag{D.1}$$

So r is

$$r = \frac{\ddot{H}}{H^3} - q + 2\frac{\dot{H}}{H^2}. \tag{D.2}$$

To replace $\dot{H}$ and $\ddot{H}$ we may make use of (2.34). Together with (6.3) it is straightforward to show that

$$r(z) = 1 - \frac{2H'}{H}(1+z) + \left\{\frac{H''}{H} + \left(\frac{H'}{H}\right)^2\right\}(1+z)^2, \tag{D.3}$$

To construct statefinder pair as a function of ρ and p let us consider a flat universe without a cosmological constant, filled with perfect fluids. Then, from a combination of Equations 2.11 and 2.12 one may write

$$\frac{\ddot{a}}{a} = -\frac{4\pi G}{3}(3p + \rho). \tag{D.4}$$

Taking the derivative and dividing by H^3 one gets

$$\frac{\dddot{a}}{aH^3} - \frac{\ddot{a}}{a}\frac{1}{H^2} = -\frac{4\pi G}{3H^3}(3\dot{p} + \dot{\rho}) \tag{D.5}$$

where the first term is defined as statefinder parameter r, second is deceleration parameter. To go further we may recall Equation 2.11,

$$H^2 = \frac{8\pi G}{3}\rho \tag{D.6}$$

and insert it in (D.5) to get

$$r = -\frac{1}{2} - \frac{3}{2}\frac{p}{\rho} - \frac{1}{2\rho H}(3\dot{p} + \dot{\rho}). \tag{D.7}$$

For a one-fluid model, we can write $(3\dot{p} + \dot{\rho}) = \left(3\frac{\partial p}{\partial \rho} + 1\right)\dot{\rho}$, use (2.14) in (D.7) and make appropriate arrangements to get

$$r = 1 + \frac{9}{2}\left(1 + \frac{p}{\rho}\right)\frac{\partial p}{\partial \rho}. \tag{D.8}$$

Following a similar approach it is straightforward to show that,

$$q = \frac{3}{2}\frac{p}{\rho} + \frac{1}{2} \tag{D.9}$$

and

$$s = \left(1 + \frac{\rho}{p}\right)\frac{\partial p}{\partial \rho}. \tag{D.10}$$

For a two-fluid model $p \to p_1 + p_2$ and $\rho \to \rho_1 + \rho_2$ and we may rewrite (D.7) as

$$\begin{aligned} r &= -\frac{1}{2} - \frac{3}{2}\frac{p_1 + p_2}{\rho_1 + \rho_2} - \frac{1}{2(\rho_1 + \rho_2)H}(3\dot{p}_1 + 3\dot{p}_2 + \dot{\rho}_1 + \dot{\rho}_2) \\ &= -\frac{1}{2} - \frac{3}{2}\frac{p_1 + p_2}{\rho_1 + \rho_2} - \frac{1}{2(\rho_1 + \rho_2)H}\left(3\frac{\partial p_1}{\partial \rho_1}\dot{\rho}_2 + 3\frac{\partial p_2}{\partial \rho_2}\dot{\rho}_2 + \dot{\rho}_1 + \dot{\rho}_2\right). \end{aligned} \tag{D.11}$$

Since (2.14) holds for both of the fluids separately

$$r = -\frac{1}{2} - \frac{3}{2}\frac{p_1 + p_2}{\rho_1 + \rho_2} - \frac{3}{2(\rho_1 + \rho_2)}\left(\left(3\frac{\partial p_1}{\partial \rho_1} + 1\right)(\rho_1 + p_1) + \left(3\frac{\partial p_2}{\partial \rho_2} + 1\right)(\rho_2 + p_2)\right), \tag{D.12}$$

which easily gives

$$r = 1 + \frac{9}{2(\rho_1 + \rho_2)}\left((\rho_1 + p_1)\frac{\partial p_1}{\partial \rho_1} + (\rho_2 + p_2)\frac{\partial p_2}{\partial \rho_2}\right), \tag{D.13}$$

and similarly

$$s = \frac{1}{(p_1 + p_2)}\left((\rho_1 + p_1)\frac{\partial p_1}{\partial \rho_1} + (\rho_2 + p_2)\frac{\partial p_2}{\partial \rho_2}\right). \tag{D.14}$$

REFERENCES

1. Misner, C., K. Thorne and J. Wheeler, *Gravitation*, Freeman, New York, 1973.

2. Einstein, A., "Kosmologische Betrachtungen zur Allgemeinen Relativitätstheorie (Cosmological Considerations in the General Theory of Relativity)", *Königlich Preussische Akademie der Wissenschaften*, February 1917.

3. Hubble, E., "A Relation Between Distance and Radial Velocity Among Extra-Galactic Nebulae", *Proceedings of the National Academy of Sciences*, Vol. 15, No. 1, pp. 168-173, January 1929.

4. Friedman, A., "Über die Krümmung des Raumes (On the Curvature of Space)", *Zeitschrift für Physik*, Vol. 10, pp. 377386, 1922.

5. Penzias, A. A. and R. W. Wilson, "A Measurement of Excess Antenna Temperature at 4080 Mc/s", *Astrophysical Journal*, Vol. 142, pp. 419-421, 1965.

6. Zwicky, F., "Die Rotverschiebung von Extragalaktischen Nebeln (The Redshift of Extragalactic Nebulae)", *Helvetica Physica Acta*, Vol. 6, pp. 110-127, 1933.

7. Zwicky, F., "On the Masses of Nebulae and of Clusters of Nebulae", *The Astrophysical Journal*, Vol. 86, No. 3, 1937.

8. Mukhanov, V. F., *Physical Foundations Of Cosmology*, Cambridge, 2005.

9. Bernabei, R., et al., "First Results from DAMA/LIBRA and the Combined Results with DAMA/NaI", *The European Physical Journal C*, Vol. 56, pp. 333-355, 2008.

10. Read, J. I., et al., "Thin, Thick and Dark Discs in ΛCDM", *Monthly Notices of the Royal Astronomical Society*, Vol. 389, pp. 1041-1052, 2008.

11. Copeland, E., M. Sami and S. Tsujikawa, "Dynamics of Dark Energy", *Interna-*

tional Journal of Modern Physics D, Vol. 15, No. 11, pp. 1753-1936, 2006.

12. Harrison, E. R., "Fluctuations at the Threshold of Classical Cosmology", *Physical Review D*, Vol. 1, pp. 2726-2730, 1970.

13. Peebles, P. J. E. and J. T. Yu, "Primeval Adiabatic Perturbation in an Expanding Universe", *The Astrophysical Journal*, Vol. 162, pp. 815-836, 1970.

14. Zel'dovich, Y. B., "A Hypothesis, Unifying the Structure and Entropy of the Universe", *Monthly Notices of the Royal Astronomical Society*, Vol. 160, pp. 1P-4P, 1972.

15. Smoot, G. F. et al., "Structure in the COBE DMR First Year Maps", *The Astrophysical Journal Letters*, Vol. 396, No. 1, pp. L1-L5, 1992.

16. de Bernardis, P., et al., "A Flat Universe from High-resolution Maps of the Cosmic Microwave Background", *Nature*, Vol. 404, pp. 955-959, 2000.

17. Lange, A. E. et al., "Cosmological Parameters from the First Results of Boomerang", *Physical Review D*, Vol. 63, No. 4, 2001.

18. Hanany, S. et al., "MAXIMA-1: A Measurement of the Cosmic Microwave Background Anisotropy on Angular Scales of 10'-5°", *The Astrophysical Journal Letters*, Vol. 545, pp. L5-L9, 2000.

19. Perkins, D., *Particle Astrophysics*, Oxford University Press, New York, 2003.

20. WMAP Science Team, "Five Year Results on the Oldest Light in the Universe", http://map.gsfc.nasa.gov/news/index.html, (03.07.2008).

21. Riess, A. G. et al., "Observational Evidence From Supernovae For An Accelerating Universe And A Cosmological Constant", *The Astronomical Journal*, Vol. 116, pp. 1009-1038, 1998.

22. Perlmutter, S. et al., "Measurements Of Ω And Λ From 42 High-Redshift Supernovae", *The Astrophysical Journal*, Vol. 517, pp. 565-586, 1999.

23. Riess, A. G. et al., "New Hubble Space Telescope Discoveries of Type Ia Supernovae at $z \geq 1$; Narrowing Constraints on the Early Behaviour of Dark Energy", *The Astrophysical Journal*, Vol. 659, pp. 98-121, 2007.

24. Astier, P., et al., "Supernova Legacy Survey: Measurement of Ω_M, Ω_Λ and w from the First Year Data Set", *Astronomy & Astrophysics*, Vol. 447, pp. 31-48, 2006.

25. Kolb, E. W. and M. S. Turner, *The Early Universe*, Westview, 1990.

26. Sahni, V., T. D. Saini, A. A. Starobinsky and U. Alam, "Statefinder – A New Geometrical Diagnostic of Dark Energy", *Pis'ma v Zhurnal Eksperimentalnoi i Teoreticheskoi Fiziki*, Vol. 77, pp. 243-248, 2003.

27. Caldwell, R. R., R. Dave and P.J. Steinhardt, "Cosmological Imprint of an Energy Component with General Equation of State", *Physical Review Letters*, Vol. 80, pp. 1582-1585, 1998.

28. Zlatev, I., L. Wang and P.J. Steinhardt, "Quintessence, Cosmic Coincidence, and the Cosmological Constant", *Physical Review Letters*, Vol. 82, pp. 896-899, 1999.

29. Steinhardt, P. J., L. Wang and I. Zlatev, "Cosmological Tracking Solutions", *Physical Review D*, Vol. 59, 123504, 1999.

30. Armendariz-Picon, C., V. Mukhanov and P.J. Steinhardt, "Dynamical Solution to the Problem of a Small Cosmological Constant and Late-Time Cosmic Acceleration", *Physical Review Letters*, Vol. 85, pp. 4438-4441, 2000.

31. Armendariz-Picon, C., T. Damour and V. Mukhanov, "k-Inflation", *Physics Letters B*, Vol. 458, pp. 209-218, 1999.

32. Chiba, T., T.Okabe and M. Yamaguchi, "Kinetically Driven Quintessence", *Phys-*

ical Review D, Vol. 62, 023511, 2000.

33. Gu, J.-A. and W.-Y.P. Hwang, "Can the Quintessence Be a Complex Scalar Field?", *Physics Letters B*, Vol. 517, pp. 1-6, 2001.

34. Boyle, L. A., R. R. Caldwell and M. Kamionkowski, "Spintessence! New models for dark matter and dark energy", *Physics Letters B*, Vol. 545, pp. 17-22, 2002.

35. Banerjee, N. and S. Das, "Spintessence: A Possible Candidate as a Driver of the Late Time Cosmic Acceleration", *Astrophysics and Space Science*, Vol. 305, pp. 25-27, 2006.

36. Caldwell, R. R., "A Phantom Menace? Cosmological Consequences of a Dark Energy Component with Super-negative Equation of State", *Physics Letters B*, Vol. 545, pp. 23-29, 2002.

37. Caldwell, R. R., M. Kamionkowski and N. N. Weinberg, "Phantom Energy: Dark Energy with $w < -1$ Causes a Cosmic Doomsday", *Physical Review Letters*, Vol. 91, 071301, 2003.

38. Kamenshchik, A., U. Moschella and V. Pasquier, "An Alternative to Quintessence", *Physics Letters B*, Vol. 511, pp. 265-268, 2001.

39. Chaplygin, S. A., "On Gas Jets", *Scientific Memoirs of Moscow University Math.-Phys. Section*, Vol. 21, pp. 1-124, 1904.

40. Bordemann, M. and J. Hoppe, "The Dynamics of Relativistic Membranes. Reduction to 2-Dimensional Fluid Dynamics", *Physics Letters B*, Vol. 317, pp. 315-320, 1993.

41. Jackiw, R. and A. P. Polychronakos, "Supersymmetric Fluid Mechanics", *Physical Review Letters*, Vol. 62, 085019, 2000.

42. Jimenez, J. B. and A. L. Maroto, "Cosmic Vector for Dark Energy", *Physical*

Review D, Vol. 78, 063005, 2008.

43. Gibbons, G. W., "Cosmological Evolution of the Rolling Tachyon", *Physics Letters B*, Vol. 537, pp. 1-4, 2002.

44. Rubano, C., P. Scudellaro and E. Piedipalumbo, "Oscillating Dark Energy: A Possible Solution to the Problem of Eternal Acceleration", *Physical Review D*, Vol. 68, 123501, 2003.

45. Li, M., "A Model of Holographic Dark Energy", *Physics Letters B*, Vol. 603, pp. 1-5, 2004.

46. Cohen, A. G., D. B. Kaplan and A. E. Nelson, "Effective Field Theory, Black Holes, and the Cosmological Constant", *Physical Review Letters*, Vol. 82, pp. 4971-4974, 1999.

47. Sotiriou, T. P. and V. Faraoni, "f(R) Theories Of Gravity", arXiv:0805.1726v2 [gr-qc], (To be published in *Reviews of Modern Physics*).

48. Carroll, S. M., V. Duvvuri, M. Trodden and M. S. Turner, "Is Cosmic Speed-up Due to New Gravitational Physics?", *Physical Review D*, Vol. 70, 043528, 2004.

49. Dvali, G., G. Gabadadze and M. Porrati, "4D Gravity on a Brane in 5D Minkowski Space", *Physics Letters B*, Vol. 485, pp. 208-214, 2000.

50. Deffayet, C., G. Dvali and G. Gabadadze, "Accelerated Universe from Gravity Leaking to Extra Dimensions", *Physical Review D*, Vol. 65, 044023, 2002.

51. Räsänen, S., "Cosmological Acceleration From Structure Formation", *International Journal of Modern Physics D*, Vol. 15, pp. 2141-2146, 2006.

52. Clifton, T., P. G. Ferreira, and K. Land, "Living in a Void: Testing the Copernican Principle with Distant Supernovae", *Physics Review Letters*, Vol. 101, 131302, 2008.

53. Caldwell, R. R. and A. Stebbins, "A Test of the Copernican Principle", *Physics Review Letters*, Vol. 100, 191302, 2008.

54. Alam, U., V. Sahni and A. A. Starobinsky, "The case for dynamical dark energy revisited", *Journal of Cosmology and Astroparticle Physics*, 06, 008, 2004.

55. Dragan, H. and A. Cooray, "Uncorrelated Estimates of Dark Energy Evolution", *Physical Review D*, Vol. 71, 023506, 2005.

56. Zhao, G., J. Xia, B. Feng and X. Zhang, "Probing Dynamics of Dark Energy with Supernova, Galaxy Clustering and the Three-Year Wilkinson Microwave Anisotropy Probe (WMAP) Observations", *International Journal of Modern Physics D*, Vol. 16, pp. 1229-1242, 2007.

57. Alam, U., V. Sahni, T. D. Saini and A. A. Starobinsky, "Exploring the Expanding Universe and Dark Energy Using the Statefinder Diagnostic", *Monthly Notices of the Royal Astronomical Society*, Vol. 344, pp. 1057-1074, 2003.

58. Starobinsky, A. A., "Future and Origin of our Universe: Modern View", *Gravitation and Cosmology*, Vol. 6, pp. 157-163, 2000.

59. Adams, F. C. and G. Laughlin, "A Dying Universe: The Long-term Fate and Evolution of Astrophysical Objects", *Reviews of Modern Physics*, Vol. 92, pp. 337-372, 1997.

60. Freese, K. and W. H. Kinney, "The ultimate fate of life in an accelerating universe", *Physic Letters B*, Vol. 558, pp. 1-8, 2003.

61. Chiueh, T. and X. G. He, "Future Island Universes in a Background Universe Accelerated by Cosmological Constant and by Quintessence", *Physical Review D*, Vol. 65, 123518, 2002.

62. Krauss, L. M. and R. J. Scherrer, "The Return of a Static Universe and the End of Cosmology", *General Relativity and Gravitation*, Vol. 39, pp. 1545-1550, 2007.

63. Nojiri, S., S. D. Odintsov and S. Tsujikawa, "Properties of Singularities in the (Phantom) Dark Energy Universe", *Physical Review D*, Vol. 71, 063004, 2005.

64. Barrow, J. D., "Sudden Future Singularities", *Classical and Quantum Gravity*, Vol. 21, No. 11, pp. L79-L83, 2004.

65. Nojiri, S. and S. D. Odintsov, "Final State and Thermodynamics of a Dark Energy Universe", *Physical Review D*, Vol. 70, 103522, 2004.

66. Binetruy, P., C. Deffayet, U. Ellwanger and D. Langlois, "Brane Cosmological Evolution in a Bulk with Cosmological Constant", *Physic Letters B*, Vol. 477, pp. 285-291, 2000.

67. Deffayet, C., "Cosmology on a Brane in Minkowski Bulk", *Physic Letters B*, Vol. 502, pp. 199-208, 2001.